Technical Report

R 820

Sponsored by

NAVAL ELECTRONIC SYSTEMS COMMAND

April 1975

CIVIL ENGINEERING LABORATORY
Naval Construction Battalion Center
Port Hueneme, CA 93043

NUCLEAR SHOCK WAVE PROPAGATION THROUGH AIR ENTRAINMENT SYSTEMS OF HARDENED FACILITIES

by

R. Fashbaugh, A. Widawsky, and D. Pal

Approved for public release; distribution unlimited.

NUCLEAR SHOCK WAVE PROPAGATION THROUGH AIR ENTRAINMENT SYSTEMS OF HARDENED FACILITIES

R. H. Fashbaugh, et al

Civil Engineering Laboratory (Navy)
Port Hueneme, California

April 1975

UNCLASSIFIED
SECURITY CLASSIFICATION OF THIS PAGE (When Data Entered)

REPORT DOCUMENTATION PAGE

READ INSTRUCTIONS BEFORE COMPLETING FORM

1 REPORT NUMBER	2 GOVT ACCESSION NO	3 RECIPIENT'S CATALOG NUMBER
TR-820	DN 144082	AD-A011 812

4 TITLE (and Subtitle)
NUCLEAR SHOCK WAVE PROPAGATION THROUGH AIR ENTRAINMENT SYSTEMS OF HARDENED FACILITIES

5 TYPE OF REPORT & PERIOD COVERED
Final; Nov 73 — May 74

6 PERFORMING ORG. REPORT NUMBER

7 AUTHOR(s)
R. H. Fashbaugh, PhD
A. Widawsky, PhD
D. Pal

8 CONTRACT OR GRANT NUMBER(s)

9 PERFORMING ORGANIZATION NAME AND ADDRESS
Civil Engineering Laboratory
Naval Construction Battalion Center
Port Hueneme, CA 93043

10 PROGRAM ELEMENT, PROJECT, TASK AREA & WORK UNIT NUMBERS
11401N; R0 001-01
63-018

11 CONTROLLING OFFICE NAME AND ADDRESS
Naval Electronic Systems Command
Washington, DC 20360

12 REPORT DATE
April 1975

13 NUMBER OF PAGES
56

14 MONITORING AGENCY NAME & ADDRESS (if different from Controlling Office)

15 SECURITY CLASS. (of this report)
Unclassified

15a DECLASSIFICATION/DOWNGRADING SCHEDULE

16 DISTRIBUTION STATEMENT (of this Report)
Approved for public release; distribution unlimited.

17 DISTRIBUTION STATEMENT (of the abstract entered in Block 20, if different from Report)

18 SUPPLEMENTARY NOTES

19 KEY WORDS (Continue on reverse side if necessary and identify by block number)
Blast, shock waves, air entrainment, explosion effects, hardening, underground structure, shock tube experimental data

PRICES SUBJECT TO CHANGE

20 ABSTRACT (Continue on reverse side if necessary and identify by block number)
An analytical study was undertaken to develop the capability of predicting nuclear shock wave propagation through air entrainment systems of hardened facilities. All solutions presented in this report are one-dimensional. Two finite-difference schemes for approximating the hyperbolic partial differential equations of fluid dynamics are used: the pseudo-viscosity scheme in a variable area Lagrange formulation, and the Lax-Wendroff two-step scheme in an Eulerian formulation. Shock wave attenuation
continued

DD FORM 1 JAN 73 1473 EDITION OF 1 NOV 65 IS OBSOLETE

UNCLASSIFIED
SECURITY CLASSIFICATION OF THIS PAGE (When Data Entered)

Block 20. Continued

due to viscous losses at ducting walls is included. A comparison of the results of the analysis with shock tube experimental data shows both formulations to be adequate. The Eulerian formulation is appropriate for constant area ducts only and is limited to air temperatures below 1,000°K. The Lagrange formulation is appropriate for constant or limited variable area ducts or a complete air entrainment system configuration. The Lagrange formulation has the capability of a simple exponential decay shock wave input to temperatures of 1,000°K or a 1-MT nuclear shock wave input to temperatures of 24,000°K.

Civil Engineering Laboratory
NUCLEAR SHOCK WAVE PROPAGATION THROUGH
AIR ENTRAINMENT SYSTEMS OF HARDENED FACILITIES
(Final), by R. H. Fashbaugh, PhD, A. Widawsky, PhD, D. Pal

TR-820 52 p. illus April 1975 Unclassified

1. Blast 2. Shock waves 3. Air entrainment 4 Explosion effects 5. Hardening
6 Underground structure 7 Shock tube experimental data

An analytical study was undertaken to develop the capability of predicting nuclear shock wave propagation through air entrainment systems of hardened facilities. All solutions presented in this report are one-dimensional. Two finite-difference schemes for approximating the hyperbolic partial differential equations of fluid dynamics are used: the pseudo-viscosity scheme in a variable area Lagrange formulation, and the Lax-Wendroff two-step in an Eulerian formulation. Shock wave attenuation due to viscous losses at ducting walls is included. A comparison of the results of the analysis with shock tube experimental data shows both formulations to be adequate. The Eulerian formulation is appropriate for constant area ducts only and is limited to air temperatures below 1,000°K. The Lagrange formulation is appropriate for constant or limited variable area ducts or a complete air entrainment system configuration. The Lagrange formulation has the capability of a simple exponential decay shock wave input to temperatures of 1,000°K or a 1-MT nuclear shock wave input to temperatures of 24,000°K.

FORWARD

This report constitutes a portion of the Project Clarinet-Sanguine facilities research program. The facilities research program was sponsored by the Earth Sciences Division of the Office of Naval Research (ONR) and by the Naval Electronic Systems Command (NAVELEX).

General direction of the program was provided by Dr. T. P. Quinn and Mr. J. L. Warner of the Earth Sciences Division of ONR. Direction, particularly in program formulation, was also provided by Dr. B. Kruger and Mr. E. Pary of NAVELEX. Mr. J. R. Allgood served as CEL project coordinator.

CONTENTS

INTRODUCTION

This report presents the results of an analytical study for predicting nuclear blast wave propagation in air entrainment systems of hardened facilities. This is the final report of the study, and the information that is presented supplements the initial report titled Shock Wave Propagation Through Air Entrainment Systems—Phase I [1].* The analytical approach to the problem is discussed in the initial report with preliminary results from two computer codes. These initial computer codes differed basically in the finite-difference method that was utilized for solution of the fundamental gas dynamics partial differential equations. One code used the pseudo-viscosity method [2] in a Lagrange formulation, and the other used a modified Lax-Wendroff two-step [2] from S. Burstein [3, 4] in an Eulerian formulation. The solutions presented in the initial report are for one-dimensional shock wave propagation in a constant area duct with the effects of viscosity at the duct wall included.

Since the initial report was issued, the computer codes have been modified considerably. The Lagrange computer code has been altered to include a variable cross-sectional area capability and wave propagation through a junction of three ducts. The Eulerian computer code has been changed to the original Lax-Wendroff two-step scheme. A modification has also been made to the Eulerian code to include pseudo-viscosity in the finite-difference equations for improved stability characteristics as recommended in References 2 and 4. Both computer codes have been refined.

Following is a description of the Lagrange and Eulerian computer codes, including the background for the finite-difference equation theory and input and output formats. The version of the Eulerian code is for shock propagation with maximum air temperatures of 1,000°K. The Lagrange code, however, includes equations of state that are appropriate for air temperatures up to 24,000°K and can be used for nuclear blast wave calculations.

LAGRANGE COMPUTER CODE DESCRIPTION

The Lagrange computer code is a one-dimensional variable area code which includes viscous effects (at a wall). The code is suitable for computation of time-dependent flows, including normal shock waves, in a single duct in which the cross-sectional area is either constant or variable, Figure 1, and in the multiple duct configuration shown in Figure 2. The basic equations and finite-difference equations used differ from those given in Reference 1 due to the inclusion of variable cross-sectional area. Two types of boundary conditions can be specified at the duct system inlet: a side-on type entrance with a surface shock wave specified that passes over the entrance (see Figure 1), or simulation of a shock wave originating at the duct inlet. In both cases the shock wave can be of constant strength or a wave with exponential pressure decay behind the shock front. For the configuration of Figure 2, a nuclear wave can be specified on the surface. The boundary condition at the exit of a duct is specified as a rigid wall except at a T-junction.

* Numbers in brackets refer to References.

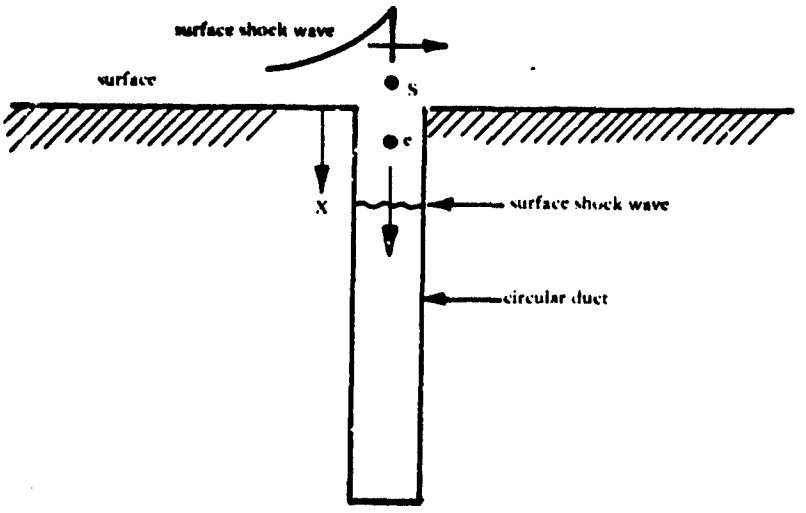

(a) Constant area duct with side-on entrance.

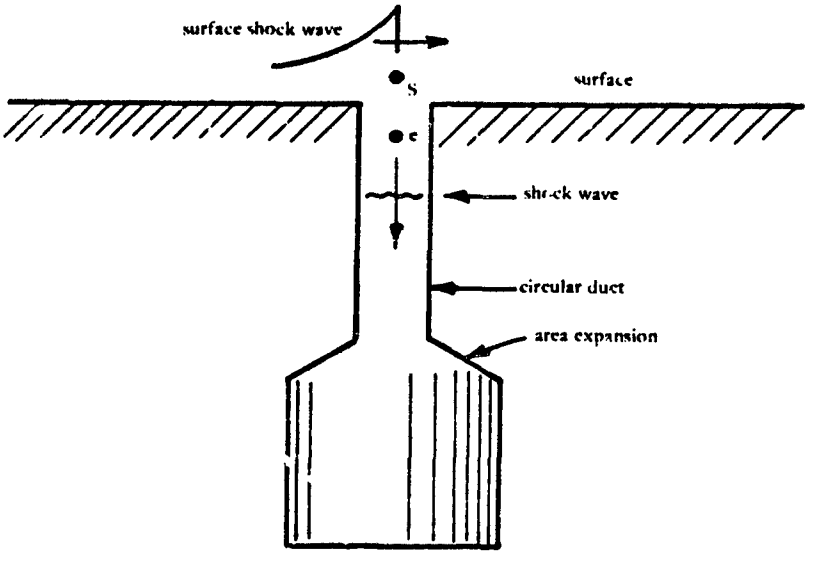

(b) Duct with area expansion and side-on entrance.

Figure 1. Single duct configurations.

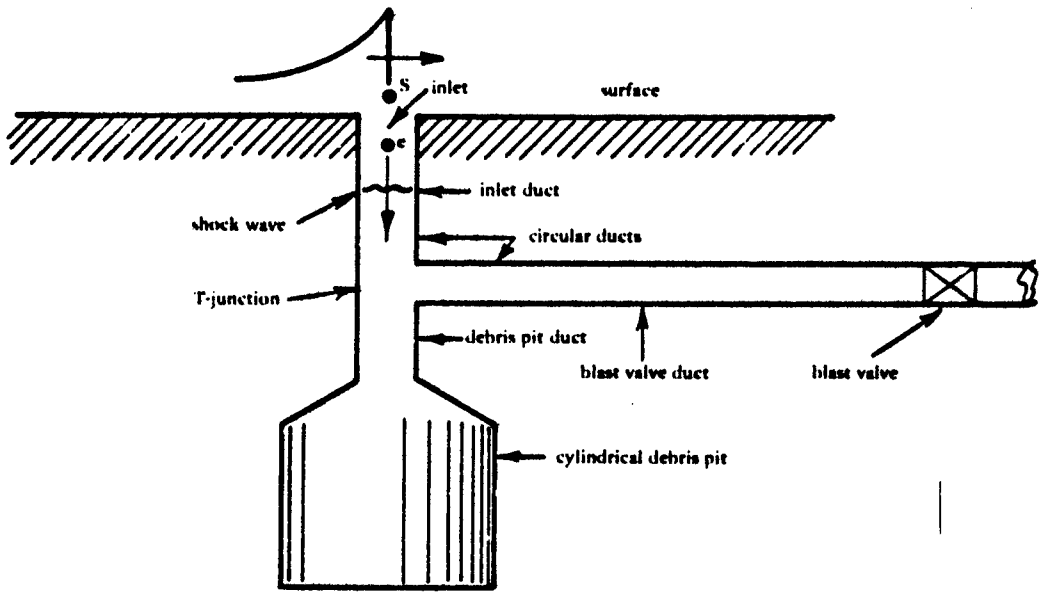

Figure 2. Typical air entrainment system.

Basic Equations

The basic differential equations are written in the Lagrange formulation with the Lagrange variable defined as

$$m = \int \frac{A}{V}\, dx \tag{1}$$

where A is the duct cross-sectional area, V is the volume per unit mass, and x is the Eulerian distance coordinate. The area A is considered a function of x. A relationship for V follows from Equation 1 that has the form

$$V = A \frac{\partial x}{\partial m} \tag{2}$$

The above equation with the definition for the velocity in Lagrange coordinates, $u = \partial x/\partial t$, yields the equation for conservation of mass, including variable area, as

$$\frac{\partial V}{\partial t} = V \frac{\partial u}{\partial x} + \frac{u V}{A}\left(\frac{dA}{dx}\right) \tag{3}$$

The inclusion of variable area does not alter the form of either the momentum equation or the energy equation. These equations are, therefore, the same as for a constant area duct, as given in Reference 1. The momentum equation is

$$\frac{\partial u}{\partial t} = -V \frac{\partial p}{\partial x} - \frac{f}{2D} u |u| \tag{4}$$

and the energy equation is

$$\frac{\partial e}{\partial t} = -p \frac{\partial V}{\partial t} + \frac{f}{2D} u^2 |u| \tag{5}$$

where p is the pressure, e the internal energy per unit mass, f a wall friction coefficient, and D the duct diameter. The system of equations is completed by the equation of state that, for the analysis presented here, takes the form

$$e = \frac{pV}{\gamma - 1} \tag{6}$$

In the above, γ is the adiabatic exponent for a real gas. The determination of the value of γ is explained in the section on equations of state. For purposes of computer computation, Equations 2, 4, 5, and 6 with the definition for the velocity u are written in finite-difference form, utilizing the pseudo-viscosity method [2] of shock wave treatment.

The Finite-Difference Equations

The finite-difference equations for the variable area computer code differ slightly from those for the constant area code reported in Reference 1. The system of equations for the variable area case is given below. In these equations superscripts represent time increments and subscripts represent space increments, so that u_j^n denotes the velocity of the j^{th} grid point of the finite-difference mesh at the n^{th} time increment. Fractional space increments represent centered or mesh midpoint values as shown in Figure 3. The finite-difference equations are:

$$u_j^{n+1/2} = u_j^n - \Delta t^{n+1/2} \left[\frac{P_{j+1/2}^n - P_{j-1/2}^n}{\frac{1}{2}(m_{j-1/2} + m_{j+1/2})} \right] A_{j-1/2}^n - \frac{f}{2D} \Delta t^{n+1/2} u_j^n |u_j^n| \tag{7a}$$

$$x_j^{n+1} = u_j^n + \Delta t^{n+1} u_j^{n+1/2} \tag{7b}$$

$$V_{j-1/2}^{n+1} = \left(\frac{x_j^{n+1} - x_{j-1}^{n+1}}{m_{j-1/2}} \right) A_{j-1/2}^{n+1} \tag{7c}$$

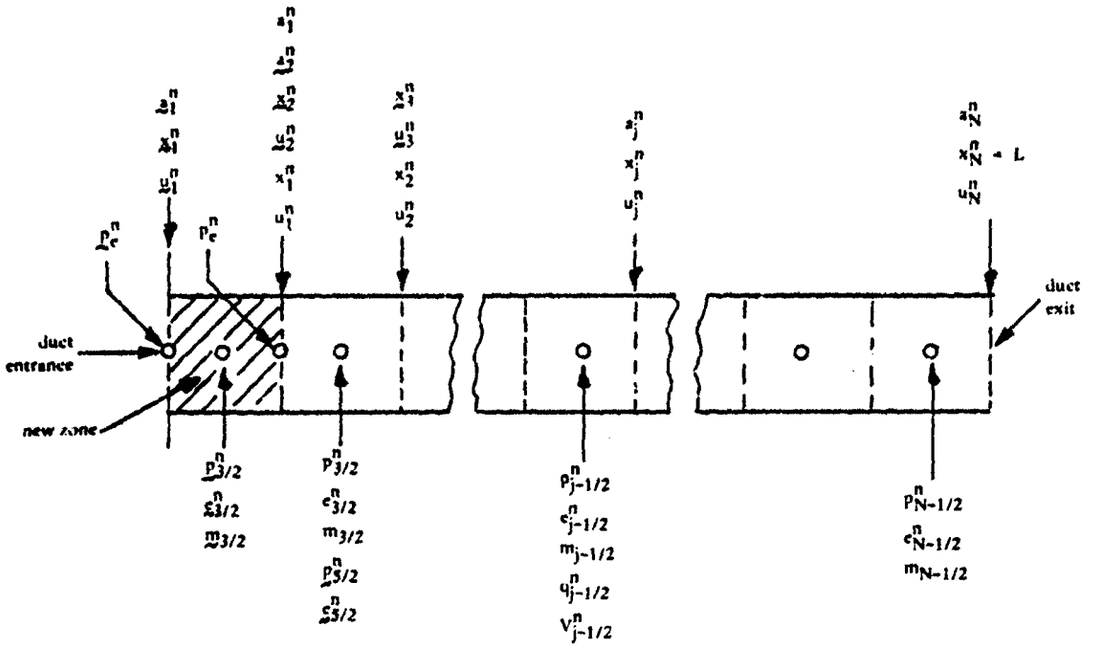

Note: $\underline{x}_1^n$, $\underline{u}_1^n$, $\underline{p}_{3/2}^n$, etc., denote parameters after a new boundary zone has been created.

Figure 3. Lagrange finite-difference grid notation.

$$q_{j-1/2}^{n+1} = a_1^2\left(\frac{x_j^{n+1} - x_{j-1}^{n+1}}{V_{j-1/2}^n}\right)^2\left(\frac{2}{V_{j-1/2}^{n+1} + V_{j-1/2}^n}\right)\left(\frac{V_{j-1/2}^n - V_{j-1/2}^{n+1}}{\Delta t^{n+1/2}}\right)^2$$
$$+ a_2\, c_{j-1/2}^n\left(\frac{x_j^{n+1} - x_{j-1}^{n+1}}{V_{j-1/2}^n}\right)\left(\frac{2}{V_{j-1/2}^{n+1} + V_{j-1/2}^n}\right)\left(\frac{V_{j-1/2}^n - V_{j-1/2}^{n+1}}{\Delta t^{n+1/2}}\right) \qquad (7d)$$

$$p_{j-1/2}^{n+1} = \left[\frac{1}{\left(\frac{\gamma+1}{\gamma-1}\right)V_{j-1/2}^{n+1} - V_{j-1/2}^n}\right]\left[2\,e_{j-1/2}^n - \left(p_{j-1/2}^n + 2\,q_{j-1/2}^{n+1}\right)\left(V_{j-1/2}^{n+1} - V_{j-1/2}^n\right)\right.$$
$$\left. + \frac{f}{D}\Delta t^{n+1}\left(u_j^{n+1/2}\right)^2 \left|u_j^{n+1/2}\right|\right] \qquad (7e)$$

$$e_{j-1/2}^{n+1} = \frac{p_{j-1/2}^{n+1} V_{j-1/2}^{n+1}}{\gamma - 1} \tag{7f}$$

$$c_{j-1/2}^{n+1} = \left(\gamma p_{j-1/2}^{n+1} V_{j-1/2}^{n+1}\right)^{1/2} \tag{7g}$$

In the above q is the artificial viscosity and $P = p + q$. The time step $\Delta t^{n+1/2}$ is the average of previously and newly calculated time steps, with Δt^{n+1} being the newly calculated time step. The symbols a_1 and a_2 are constants.

The stability criterion that must be satisfied for the finite-difference equations to be stable is:

$$\frac{c\,\Delta t}{\Delta x}(1 + 2a_2) + 4a_1^2\left(\frac{\Delta V}{V}\right) \leq 1 \tag{8}$$

The Boundary Conditions

Inlet Boundary Conditions. In the Lagrange code two types of duct inlet boundary conditions can be specified: a side-on type entrance or simulation of a shock wave originating at a duct inlet. In a Lagrange formulation it is only necessary to specify the pressure at the duct inlet and the initial state of the gas in the duct to produce a shock wave in the duct. Values of other parameters, such as velocity, density, and internal energy behind the shock wave, are determined by the conservation equations and equation of state. Since the zones of the finite-difference grid are not stationary in this formulation, a new zone needs to be established periodically at the duct entrance to allow for mass inflow. In establishing this new zone two state parameters have to be specified; in this case the state parameters used are the pressure and internal energy. When a shock wave of constant strength is established at the duct entrance, the internal energy and pressure for a new zone is determined uniquely by the shock Mach number. With the inlet shock Mach number specified, the initial inlet pressure is determined from the relation

$$p(0,0) = p_a\left[(1 + \mu^2)M_s^2 - \mu^2\right] \tag{9}$$

where $p(0,0)$ = pressure at $x = 0$ for $t = 0$.

M_s = shock Mach number

p_a = ambient pressure

$\mu^2 = (\gamma - 1)/(\gamma + 1)$

When specifying a shock of constant strength, Equation 9 is used for $t \geq 0$.

For shock waves with pressure decay following the shock front the duct inlet pressure for $t > 0$ is approximated by,

$$p(0,t) = p_a + [p(0,0) - p_a]\,e^{-t/t_i} \tag{10}$$

where t_i is the initial slope time intercept for the wave. This simple form for the inlet pressure is adequate for simulating shock waves that do not have a significant negative pressure phase, e.g., TNT blast waves outside of the fireball region [5] and experimental shock tube waves after rarefaction catchup has occurred

[1, 6]. To simulate nuclear blast waves where a significant negative pressure phase occurs Equation 10 is replaced by more appropriate relationships such as are given in Reference 7. These relationships for a surface wave that are used in side-on entrance calculations are given below:

$$P_s = P_a + P_{so}\left(A_1 e^{-b_1 \tau} + A_2 e^{-b_2 \tau} + A_3 e^{-b_3 \tau}\right)(1 - \tau) \tag{11}$$

where $\tau = (t - t_s)/D_p^+$

t_s = shock arrival time

D_p^+ = duration of positive pressure phase

P_{so} = shock peak overpressure at $t = t_s$

The quantities A_1, A_2, A_3, b_1, b_2, and b_3 are constants for which values are given in Reference 7 for a 1-Mt nuclear burst. In addition to a relationship for the surface pressure, p_s, relationships for the dynamic pressure, Q_s, and temperature, T_s, are required.

$$Q_s = Q_{so}\left(A_4 e^{-b_4 \omega} + A_5 e^{-b_5 \omega}\right)(1 - \omega)^2 \tag{12}$$

$$T_s = T_{so}\left(\frac{t}{t_s}\right)^{b_6} \tag{13}$$

where $\omega = (t - t_s)/D_u^+$

D_u^+ = duration of positive velocity phase

Q_{so} = peak dynamic pressure at $t = t_s$

T_{so} = shock temperature at $t = t_s$

The quantities A_4, A_5, b_4, b_5, and b_6 are constants for which values are given in Reference 7. Equations 11, 12, and 13 completely define the surface conditions in the air above an inlet from which other variables can be obtained. The total enthalpy is required for side-on entrance simulation and is defined as

$$h_{ts} = e_s + \frac{P_s}{\rho_s} + \frac{1}{2} u_s^2 \tag{14}$$

The density ρ_s is computed using Equations 11 and 13, and the equation of state,

$$\rho_s = \frac{P_s}{Z_s R T_s} \tag{15}$$

The parameter Z_s is a function of temperature and density and is determined as explained in the section on equations of state. The internal energy, e_s, is determined from

$$e_s = \frac{P_s}{\rho_s(\gamma_s - 1)} \tag{16}$$

where γ_s is also a function of temperature and density. The particle velocity, u_s, is computed using Equation 12 and the definition

$$u_s = \sqrt{\frac{2Q_s}{\rho_s}} \tag{17}$$

Simulation of a side-on type entrance is achieved by using Equations 9 and 10 or 11 to compute the surface pressure, p_s, (point s on Figure 2) and then calculating the duct inlet pressure (point e on Figure 2) from the empirical relation,

$$p_e = p_a + 0.969(p_s - p_a)^{0.804} \tag{18}$$

The above relationship was obtained from data in Reference 8. (In the computer program Equation 18 is input in table form.) When a new zone is formed at the duct entrance, the internal energy of the new zone is determined by assuming the total enthalpy at points s and e are equal. This assumption yields,

$$e_e = \frac{1}{\gamma_e}\left(h_{ts} - \frac{1}{2}u_e^2\right) \tag{19}$$

where h_{ts} is the total enthalpy at point s. The equation of state has been used in obtaining Equation 19. The value of h_{ts} is known since values for all shock parameters are known at point s; it is given by Equation 14. The value of u_e is, however, unknown and is approximated by the value calculated during the previous time cycle. An iteration technique could be used to improve the value for u_e, but a comparison of computed results with experimental data showed this to be unnecessary (Reference 1). The pressure in the new zone is initially assumed as the mean between the inlet pressure, p_e, and the pressure in the second zone. The pressure, internal energy, and velocity completely define the initial state for the new zone. This approximate method for establishing a new inlet zone to allow mass inflow yields a result for the shock peak pressure that is approximately 5% high and a shock speed that is approximately 2% high. Rezoning methods will be discussed in more detail in a separate section below.

Some discussion is in order concerning the appropriateness of Equation 18 in defining the flow losses at the duct inlet. Equation 18 defines the static pressure change through the inlet and agrees essentially with data from other sources than BRL, e.g., TRW Systems investigation, IITRI investigation, and the B.E.L. Deckler and D. H. Male investigation, References 9, 10, and 11, respectively. Using the second law of thermodynamics an expression characterizing the inlet loss can be derived if γ and Z are assumed constant from point s to point e (Figure 2). This loss is measured by the entropy change and is given by

$$S_e - S_s = Z R \ln\left[\left(\frac{p_e}{p_s}\right)^{1/(\gamma-1)}\left(\frac{\rho_e}{\rho_s}\right)^{\gamma/(\gamma-1)}\right] \tag{20}$$

where S_s and S_e are the entropy at point s and point e, respectively, and Z and γ are the values at point s. An alternate form for Equation 20 in terms of the stagnation pressures at points s and e is

$$S_e - S_s = Z R \ln\left(\frac{p_{ss}}{p_{se}}\right) \tag{21}$$

Examination of Equations 20 and 21 clearly shows that the flow loss through an inlet or junction is determined solely by the stagnation pressure change; specification of static pressure change only, as by Equation 18, neglects the density change effects. For constant normal shock waves specification of the static pressure above is correct since all other parameters, such as density and stagnation pressure, are determined uniquely from the static pressure behind the shock wave. However, for shock waves that have a rarefaction behind the shock surface or in which the air behind the shock surface is heated by radiation, e.g., a nuclear wave, the density change should be included as indicated in Equation 20. Data currently available do not allow for inclusion of density effects except for a limited amount of data in Reference 9. To specify the losses at an inlet more accurately than is done by Equation 18 additional data are required in which the surface density (or a related state variable such as temperature) is varied independently of the surface pressure.

T-Junction Boundary Condition. The T-junction (Figures 2 and 4) for the Lagrange coordinate system is considered as three separate ducts joined through appropriate boundary conditions at the end of each duct. The finite-difference grid in each of the ducts is moving, which requires the boundary zones to be modified at each calculation cycle. For example, with the shock wave moving down duct 1 into ducts 2 and 3, as shown in Figure 4, the boundary zone of duct 1 is moving into the junction, and the boundary zones of ducts 2 and 3 are moving away from the junction; this requires the mass to be removed from the duct 1 boundary zone and added to the boundary zones of ducts 2 and 3. This boundary zone modification (changing the mass of the zone) is done in a manner that satisfies conservation of mass. In addition to conservation of mass, the conservation of energy and the flow losses through the junction are also considered. Conservation of energy is provided by assuming a quasi-steady state flow exists which allows use of a constant total enthalpy; this is the same method previously described that is used in determining flow through a duct inlet. The flow losses through the junction are determined from experimental data (Reference 8).

The computation procedure used at the T-junction is an iterative one. A value for the static pressure at the exit to duct 1, $p^n_{1,N}$ in Figure 4, is determined during each calculation cycle, which allows satisfaction of the following conservation of mass relations:

$$\delta^n = \Delta m_1 + \Delta m_2 + \Delta m_3$$

$$|\delta^n| \leq m^n_1 \times 10^{-7} \tag{22}$$

where Δm_1, Δm_2, and Δm_3 are the changes in the mass of the boundary zones of ducts 1, 2, and 3 during the n^{th} time cycle, respectively, and m^n_1 is the total mass of the boundary zone of duct 1. Through an iteration procedure the deviation of δ^m from zero is determined to within a small bound. The following auxiliary relationships, in finite-difference form, are used to determine Δm_1.

$$\Delta m_1 = -A_1 \rho^{n+1}_{1,N-1/2} \left(x^{n+1}_{1,N} - L_1 \right) \tag{23a}$$

$$x^{n+1}_{1,N} = x^n_{1,N} + \Delta t^{n+1} u^{n+1/2}_{1,N} \tag{23b}$$

$$u^{n+1/2}_{1,N} = u^n_{1,N} + \Delta t^{n+1/2} a^n_{1,N} \tag{23c}$$

$$a^n_{1,N} = 2 A_1 \left(\frac{p^n_{1,N-1/2} - p^n_{1,N}}{m^n_1} \right) \tag{23d}$$

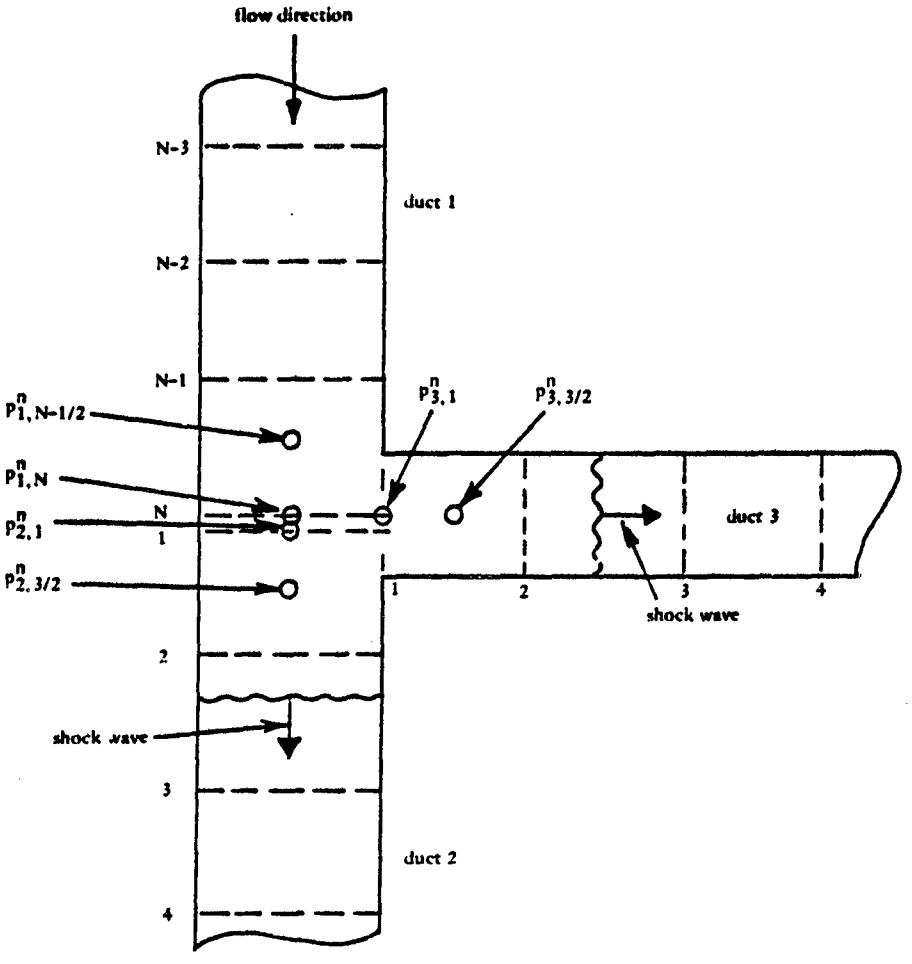

Figure 4. T-junction finite-difference grid notation.

$$V^{n+1}_{1,N-1/2} = \left(\frac{x^{n+1}_{1,N} - x^{n+1}_{1,N-1}}{m^n_1}\right)A_1 \qquad (23e)$$

$$\rho^{n+1}_{1,N-1/2} = \frac{1}{V^{n+1}_{1,N-1/2}} \qquad (23f)$$

In the above, L_1 is the length of duct 1, A_1 is the cross-sectional area of the boundary zone, and other symbols are as previously defined. The acceleration of the N^{th} interface of duct 1 at the n^{th} calculation cycle (or n^{th} time step) is represented by $a^n_{1,N}$.

The inlet pressures to ducts 2 and 3, $p^n_{2,1}$ and $p^n_{3,1}$, respectively, are determined from the exit pressure of duct 1 through the data of Reference 8. Losses are accounted for in the same manner as previously discussed for the inlet simulation of duct 1, i.e., through change in static pressure following a normal shock wave propagating through the junction. The pressures $p^n_{2,1}$ and $p^n_{3,1}$ depend upon $p^n_{1,N}$ through relationships similar to Equation 19 but with different empirical constants. (In the computer program these relationships are input in table form.) The mass transferred from duct 1 to duct 2, Δm_2, is determined in terms of $p^n_{2,1}$ (and, therefore, in terms of $p^n_{1,N}$ implicitly) by the relationships given below. The mass transferred to duct 3, Δm_3, is determined by relationships of identical form but with $p^n_{3,1}$ in place of $p^n_{2,1}$ and index 2 replaced by 3 in other appropriate symbols.

$$\Delta m_2 = A_2 \rho^{n+1}_{2,3/2} x^{n+1}_{2,1} \tag{24a}$$

$$x^{n+1}_{2,1} = x^n_{2,1} + \Delta t^{n+1} u^{n+1/2}_{2,1} \tag{24b}$$

$$u^{n+1/2}_{2,1} = u^n_{2,1} + \Delta t^{n+1/2} a^n_{2,1} \tag{24c}$$

$$a^n_{2,1} = 2A_2\left(\frac{P^n_{2,3/2} - p^n_{2,1}}{m^n_2}\right) \tag{24d}$$

$$V^{n+1}_{2,3/2} = \left(\frac{x^{n+1}_{2,2} - x^{n+1}_{2,1}}{m^n_2}\right)A_2 \tag{24e}$$

$$\rho^{n+1}_{2,3/2} = \frac{1}{V^{n+1}_{2,3/2}} \tag{24f}$$

In the above, A_2 is the cross-sectional area of the boundary zone of duct 2, $x^{n+1}_{2,2}$ is determined using Equation 7b, and $P^n_{2,3/2}$ represents $p^n_{2,3/2} + q^n_{2,3/2}$. Utilizing Equations 23, 24, and the equivalent of Equations 24a through 24f for Δm_3, Equation 22 is satisfied by iteration of the pressure $p^n_{1,N}$ for each calculation cycle.

Since mass is added to the boundary zones of ducts 2 and 3 from duct 1, the mass of the three zones involved is adjusted at each calculation cycle. In addition, the internal energy and static pressure of the boundary zones of ducts 2 and 3 are adjusted to account for effects of the internal energy of the added mass. Assuming quasi-steady state flow, and therefore, constant total enthalpy, and using a mass weighted averaging method yields the following relationships for the adjusted variables.

$$\mathcal{E}^{n+1}_{1,N-1/2} = e^{n+1}_{1,N-1/2} \tag{25a}$$

$$h^{n+1}_{t1} = \mathcal{E}^{n+1}_{1,N-1/2} + \frac{p^{n+1}_{1,N-1/2}}{\rho^{n+1}_{1,N-1/2}} + \frac{1}{2}\left(u^{n+1}_{1,N}\right)^2 \tag{25b}$$

$$\Delta e_2 = h_{t1}^{n+1} - \frac{p_{2,3/2}^{n+1}}{\rho_{2,3/2}^{n+1}} - \frac{1}{2}\left(u_{2,1}^{n+1}\right)^2 \tag{25c}$$

$$\Delta e_3 = h_{t1}^{n+1} - \frac{p_{3,3/2}^{n+1}}{\rho_{3,3/2}^{n+1}} - \frac{1}{2}\left(u_{3,1}^{n+1}\right)^2 \tag{25d}$$

$$m_1^{n+1} = m_1^n + \Delta m_1 \tag{25e}$$

$$m_2^{n+1} = m_2^n + \Delta m_2 \tag{25f}$$

$$m_3^{n+1} = m_3^n + \Delta m_3 \tag{25g}$$

$$\underline{e}_{2,3/2}^{n+1} = \left(m_2^n e_{2,3/2}^{n+1} - \Delta m_2 \Delta e_2\right) \frac{1}{m_2^{n+1}} \tag{25h}$$

$$\underline{e}_{3,3/2}^{n+1} = \left(m_3^n e_{3,3/2}^{n+1} - \Delta m_3 \Delta e_3\right) \frac{1}{m_3^{n+1}} \tag{25i}$$

$$\underline{p}_{1,N-1/2}^{n+1} = p_{1,N-1/2}^{n+1} \tag{25j}$$

$$\underline{p}_{2,3/2}^{n+1} = (\gamma - 1)\underline{e}_{2,3/2}^{n+1} \rho_{2,3/2}^{n+1} \tag{25k}$$

$$\underline{p}_{3,3/2}^{n+1} = (\gamma - 1)\underline{e}_{3,3/2}^{n+1} \rho_{3,3/2}^{n+1} \tag{25l}$$

The barred quantities are adjusted variables, and values for $p_{1,N-1/2}^{n+1}$, $e_{1,N-1/2}^{n+1}$, $p_{2,3/2}^{n+1}$, $e_{2,3/2}^{n+1}$, $p_{3,3/2}^{n+1}$, and $e_{3,3/2}^{n+1}$ are determined from Equations 7e and 7f. Values for other variables are obtained from Equations 23 and 24.

The mass of the boundary zone of duct 1 increases and the mass of the boundary zones of ducts 2 and 3 decrease. Therefore, a limit has to be set on the change in the mass of these zones. A rezoning method is used that merges the boundary zone of duct 1 with the adjacent zone when the boundary zone mass becomes one half of its original (cycle 1) value. The boundary zones of ducts 2 and 3 are divided into two zones of equal mass when their mass becomes double the original (cycle 1) value. This rezoning method will be discussed in more detail in the section on duct rezoning.

Equations 23 through 25 are restricted in use to the flow and shock wave directions shown in Figure 4, i.e., flow from duct 1 into ducts 2 and 3. This is the initial flow pattern for a shock propagating into the system inlet. Shock reflections from the debris pit end and/or the blast valve (Figure 2) can cause the flow directions to change. The computer code subroutine is written for the case given in detail above, and, therefore, computations will terminate when a reflected shock wave arrives at the T-junction. Subroutines can, however, easily be added to the computer code to compute propagation of reflected shock waves through this junction since the computation method is similar to the case given here; only the directions of mass transfer and flow loss relationships change. The main limitation this restriction places on the use of the computer code in its present form is the ability to compute long enough in time to allow flow reversal in both

the duct to the debris pit and the duct to the blast valve. For example, if the blast valve duct is long compared to the debris pit duct, a reflected shock wave from the debris pit could arrive at the T-junction before the shock wave in the blast valve duct arrives at the valve. This limitation is overcome by computing two geometries, the desired geometry to obtain the debris pit solution and a second geometry that replaces the debris duct with a very long constant area duct to obtain the blast valve duct solution. This method is relatively accurate since the debris pit flow does not significantly affect the flow in the blast valve duct until a reflected shock arrives at the T-junction (see Results Section). In this manner the primary problem is solved which is the temperature and pressure distribution in the ducting system up to the time flow reversal occurs at the blast valve.

Duct Exit Boundary Conditions. The boundary condition at the exit end of ducts 2 and 3 is considered a closed-end condition. In finite-difference form the boundary conditions are written,

$$a^n_{2,N} = 0 \tag{26a}$$

$$a^n_{3,N} = 0 \tag{26b}$$

where $a^n_{2,N}$ and $a^n_{3,N}$ are the accelerations of the N^{th} or last interface of ducts 2 and 3, respectively.

The Finite-Difference Grid Rezoning Methods

Changing the finite-difference grid in each duct by adding or combining zones and renumbering the grid system—denoted rezoning—is required periodically during a calculation to allow mass flow into or out of a duct. For the configuration of Figure 2 rezoning is required for calculating mass flow into duct 1 and also through the T-junction. Another type of rezoning that is employed in the Lagrange computer code is the removal of excessively compressed zones by combining these zones with an adjacent zone. This is necessary to control the minimum size of the time step, which is determined for each calculation cycle by the smallest zone.

Inlet Duct Rezoning. At the inlet of duct 1 a new boundary zone is established whenever the first interface has moved a distance equivalent to the mass of the initial boundary zone. To establish this zone the state of the gas at the zone center, the velocity of the zone interface, and the zone size have to be specified. The zone mass is determined from the gas state and zone size, and the acceleration of the interface is determined from the zone pressure with adjacent zone pressures. The specification of initial values for these quantities is necessarily approximate; however, test calculations with the computer code show that rezoning causes the shock pressure to be within 5% of the correct value. The computed shock pressure is always above the correct value, yielding a conservative answer.

The basic assumptions that are made to establish the initial values for the new zone parameters are, referring to Figure 3, $\underset{\sim}{a}^n_2 = 0$ and $\underset{\sim}{m}_{3/2} = m_{3/2}$. Neglecting the friction term (which is small) in the first part of Equation 7a and using the following relationship for the acceleration of the boundary interface,

$$\underset{\sim}{a}^n_1 = \left(\underset{\sim}{p}^n_e - \underset{\sim}{p}^n_{3/2}\right)\left(\frac{2A_1}{\underset{\sim}{m}_{3/2}}\right) \tag{27}$$

yields the relationship

$$\underset{\sim}{p}^n_{3/2} = p^n_{3/2} \tag{28a}$$

$$\underline{a}_3^n = a_1^n \tag{28b}$$

Again, $P_{3/2}^n = p_{3/2}^n + q_{3/2}^n$. The above-mentioned assumptions, therefore, imply that the acceleration of the boundary interface does not change when a new boundary zone is created. Of several rezoning methods tested the above yielded the most accurate results.

The criterion for establishment of the new boundary zone is

$$\dot{x}_o \geq x_1^n \tag{29}$$

where

$$x_o = \frac{2\, m_{3/2}}{A_1}\left[\frac{(\gamma - 1)e_c^n}{p_e^n + p_{3/2}^n}\right] \tag{30}$$

$$e_e^n = \frac{1}{\gamma}\left[h_{ts} - \frac{1}{2}\left(u_1^n\right)^2\right] \tag{31}$$

and h_{ts} is given by Equation 14.

The initial values of parameters for the new boundary zone of duct 1 based on Equations 28 are as follows:

$$\underline{u}_1^n = u_1^n \tag{32a}$$

$$\underline{x}_1^n = 0 \tag{32b}$$

$$\underline{p}_{3/2}^n = \frac{1}{2}\left(p_e^n + p_{3/2}^n\right) \tag{32c}$$

$$\underline{P}_{3/2}^n = P_{3/2}^n \tag{32d}$$

$$\underline{e}_{3/2}^n = e_e^n \tag{32e}$$

$$\underline{V}_{3/2}^n = \frac{(\gamma - 1)\underline{e}_{3/2}^n}{\underline{p}_{3/2}^n} \tag{32f}$$

$$\underline{m}_{3/2} = \frac{A_1 \underline{x}_2^n}{\underline{V}_{3/2}^n} \tag{32g}$$

When initial values have been established for the new zone parameters, all the zones of the finite-difference grid are renumbered to include this additional zone.

T-Junction Rezoning. Since mass is flowing through the T-junction, the boundary zones at this junction change mass with each calculation cycle. The exit boundary zone of duct 1 decreases in mass, and the entrance boundary zones of ducts 2 and 3 increase in mass. This change in zone mass eventually requires

that the boundary zones be altered. The procedure that is used in the computer code is similar to the duct 1 inlet rezoning described above, i.e., a new zone is established periodically, and the finite-difference grid renumbered accordingly. The exit boundary zone of duct 1 is combined with its adjacent zone to form a new boundary zone when its mass becomes one half of its original mass. The inlet boundary zones of ducts 2 and 3 are split to form two zones when their mass becomes double the original mass.

The criterion for establishment of a new exit zone for duct 1 is

$$m_{N-1/2} \leq \frac{1}{2} m^1_{N-1/2} \tag{33}$$

where $m^1_{N-1/2}$ represents the zone mass at time zero. The relationships for establishing values of parameters for the new zone are given below.

$$\underline{\varepsilon}^n_{N-1/2} = \frac{\varepsilon^n_{N-1/2} m_{N-1/2} + \varepsilon^n_{N-3/2} m_{N-3/2}}{\underline{m}_{N-1/2}} \tag{34a}$$

$$\underline{p}^n_{N-1/2} = \frac{1}{2}\left(p^n_{N-1/2} + p^n_{N-3/2}\right) \tag{34b}$$

$$\underline{m}_{N-1/2} = m_{N-1/2} + m_{N-3/2} \tag{34c}$$

$$\underline{x}^n_N = x^n_N \tag{34d}$$

$$\underline{u}^n_N = u^n_N \tag{34e}$$

$$\underline{V}^n_{N-1/2} = \frac{A_1\left(x^n_N - x^n_{N-2}\right)}{\underline{m}_{N-1/2}} \tag{34f}$$

$$\underline{\rho}^n_{N-1/2} = \frac{(\gamma-1)\underline{\varepsilon}_{N-1/2}}{\underline{V}^n_{N-1/2}} \tag{34g}$$

In the above, $\underline{\varepsilon}^n_{N-1/2}$, etc., represents the new zone value.

The criterion for establishment of a new entrance zone for duct 2 or 3 is

$$m_{3/2} \geq 2\, m^1_{3/2} \tag{35}$$

where $m^1_{3/2}$ represents the zero time value. The relationships for establishing the two new entrance zones are as follows.

$$\underline{x}^n_1 = x^n_1 \tag{36a}$$

$$\underline{u}^n_1 = u^n_1 \tag{36b}$$

$$\underset{\sim}{u}_2^n = \frac{1}{2}\left(u_1^n + u_2^n\right) \tag{36e}$$

$$\underset{\sim}{m}_{3/2} = \frac{1}{2} m_{3/2} \tag{36d}$$

$$\underset{\sim}{m}_{5/2} = \frac{1}{2} m_{3/2} \tag{36e}$$

$$\underset{\sim}{\varepsilon}_{3/2}^n = \varepsilon_{3/2}^n \tag{36f}$$

$$\underset{\sim}{P}_{3/2}^n = \frac{1}{2}\left(p_c^n + P_{3/2}^n\right) \tag{36g}$$

$$\underset{\sim}{P}_{5/2}^n = \frac{1}{4}\left(3P_{3/2}^n + P_{5/2}^n\right) \tag{36h}$$

$$\underset{\sim}{q}_{3/2}^n = q_{3/2}^n \tag{36i}$$

$$\underset{\sim}{p}_{3/2}^n = \underset{\sim}{P}_{3/2}^n - \underset{\sim}{q}_{3/2}^n \tag{36j}$$

$$\underset{\sim}{V}_{3/2}^n = \frac{(\gamma - 1)\underset{\sim}{\varepsilon}_{3/2}^n}{\underset{\sim}{p}_{3/2}^n} \tag{36k}$$

$$\underset{\sim}{x}_2^n = \underset{\sim}{x}_1^n + \frac{\underset{\sim}{m}_{3/2}\underset{\sim}{V}_{3/2}^n}{A_2} \tag{36l}$$

$$\underset{\sim}{x}_3^n = \underset{\sim}{x}_2^n \tag{36m}$$

$$\underset{\sim}{V}_{5/2}^n = \frac{A_2\left(\underset{\sim}{x}_3^n - \underset{\sim}{x}_2^n\right)}{\underset{\sim}{m}_{5/2}} \tag{36n}$$

$$\underset{\sim}{p}_{5/2}^n = \frac{(\gamma - 1)\underset{\sim}{\varepsilon}_{5/2}^n}{\underset{\sim}{V}_{5/2}^n} \tag{36o}$$

$$\underset{\sim}{q}_{5/2}^n = \underset{\sim}{P}_{5/2}^n - \underset{\sim}{p}_{5/2}^n \tag{36p}$$

These relationships apply to establishing new zones at the entrance of both ducts 2 and 3.

Rezoning to Reduce Running Time. To aid in reducing computer running time it is expedient to avoid zones becoming excessively compressed. The calculation time step is based upon the smallest or most highly compressed zone. When the time step becomes too small, it is, therefore, necessary to remove the

smallest zone (the zone upon which the time step is based) by combining this zone with an adjacent zone. A criterion for removal of the small zone is established, and relationships for combining this zone with an adjacent zone are formulated.

The criterion for removal of an excessively compressed zone is

$$\Delta t^{n+1/2} < \frac{1}{2}\,\Delta t^{0} \tag{37}$$

where Δt^{0} is the initial or zero time value of $\Delta t^{n+1/2}$. The relationships to establish a new zone comprised of the zone being removed and an adjacent zone, with x_j^n the location of interface between the zones, are:

$$\underline{x}_j^n = x_{j+1}^n \tag{38a}$$

$$\underline{u}_j = u_{j+1}^n \tag{38b}$$

$$\underline{m}_{j-1/2} = m_{j-1/2} + m_{j+1/2} \tag{38c}$$

$$\underline{V}_{j-1/2}^n = \frac{A_j^n\left(\underline{x}_j^n - x_{j-1}^n\right)}{\underline{m}_{j-1/2}} \tag{38d}$$

$$\underline{e}_{j-1/2}^n = \frac{e_{j-1/2}^n\, m_{j-1/2} + e_{j+1/2}^n\, m_{j+1/2}}{\underline{m}_{j-1/2}} \tag{38e}$$

$$\underline{p}_{j-1/2}^n = \frac{p_{j-1/2}^n\, m_{j-1/2} + p_{j+1/2}^n\, m_{j+1/2}}{\underline{m}_{j-1/2}} \tag{38f}$$

$$\underline{q}_{j-1/2}^n = \frac{1}{2}\left(q_{j-1/2}^n + q_{j+1/2}^n\right) \tag{38g}$$

$$\underline{p}_{j-1/2}^n = \underline{p}_{j-1/2}^n + \underline{q}_{j-1/2}^n \tag{38h}$$

The quantities $\underline{x}_j^n$, $\underline{u}_j^n$, etc., represent values of parameters for the newly created zone, and A_j^n is the cross-sectional area at the interface of the zones being combined. A zone is removed whenever the minimum time step, $\Delta t^{n+1/2}$, based on that zone becomes smaller than one half the value of $\Delta t^{n+1/2}$ at time zero as expressed by Equation 37.

The Equation of State Options

Two equations of state subroutines are available in the Lagrange computer code: (a) the equation of state for an ideal gas that is accurate for temperatures up to 1,000°K, and (b) a real gas equation of state that is accurate for temperatures up to 24,000°K. The basic theory upon which these subroutines are based is given below.

The Perfect Gas Equation of State. The equation of state for an ideal gas can be written in the form:

$$p = \frac{RT}{V} \tag{39}$$

where **p** is the pressure, **R** the particular gas constant, **T** the absolute temperature, and **V** the specific volume. Because of the computational advantages offered by the use of Equation 39, most problems of shock transmission through gases are solved using the ideal gas law. Moreover, the ideal gas law yields simple analytical relationships between the various shock parameters. The thermally and calorically perfect gas is, however, an idealization, and real gases, depending on their temperature and pressure, will deviate from it to a varying degree. It has been noted from experience (References 12 and 13) that the ideal gas law predicts the shock flow parameters with good accuracy up to temperatures of 1,000°K. However, at higher temperatures, the number of particles per unit mass and, hence, the average molecular weight of the gas may change due to molecular dissociation, chemical reactions, and ionization. Thus, when computing flow parameters for shocks through gases at high temperatures and moderately high pressures, the ideal gas equation must be modified to include the contributions by additional degrees of freedom to the energy of the gas molecules that were not excited at low temperatures.

The Real Gas Equation of State. The translational and rotational degrees of freedom of molecules are excited at very low temperatures up to the order of 10°K, whereas the molecular vibrations absent in monotonic gases are fully excited at much higher temperatures of the order of 2,230°K for O_2 and 3,340°K for N_2. The contribution by the vibrational excitation at lower temperatures can be computed by the method of partitions described in Reference 12. Thus, for a diatonic gas with no molecular dissociation and ionization present, γ, the adiabatic exponent, is 7/5 with unexcited vibrational mode, while with fully excited molecular vibrations $\gamma = 9/7$. For a monotonic gas γ holds a constant value of 5/3.

It should be stated here that the temperature range for which the molecular vibrations stay fully excited is not very wide. This is because the molecular dissociation and chemical reactions frequently begin at temperatures at which the molecular vibrations contribution to internal energy reaches its classical limiting value. At temperatures of the order of several thousand degrees (3,000°K), the molecules of diatonic gases dissociate into atoms. The process of dissociation of a molecule requires a large amount of energy, thus affecting the thermodynamic properties of the gases appreciably. At standard atmospheric density, molecular dissociation in air is noticeable at 2,980°K due primarily to breaking up of the O_2 molecule. The internal energy of a partially dissociated gas is the sum of the energy of the undissociated molecules, the energy contained in dissociated atoms, and the energy required to dissociate unexcited molecules. Because of the high energy required to dissociate a molecule into its atoms, the energy of dissociated gas, even for small degrees of dissociation, is very much greater than that in the absence of dissociation. For monotonic gases effects due to molecular dissociation are absent.

Another factor that changes the thermodynamic properties of a mixture of gases, such as air at high temperatures, is the occurrence of chemical reactions between its constituents. Air at temperatures above 1,500°K undergoes oxidation of a portion of its nitrogen to form nitric oxide. This is a reversible reaction and requires a high activation energy (21.4 kcal/mole). The time to attain equilibrium is very high at temperatures below 1,500°K; however, at temperatures of the order of 3,000°K and above the chemical equilibrium is reached in 10^{-4} seconds or less. In other words, the chemical composition of air around 3,000°K and above contains nitric oxide as one of its components, which changes the thermodynamic properties of air somewhat.

Next, ionization of atoms or molecules of gases in air begins around 8,000°K. The degree of ionization increases with temperature. When the air temperature is of the order of 30,000°K, all of its atoms are singly ionized. At temperatures above 30,000°K, the air undergoes second followed by third ionization processes. Since this investigation deals with air temperatures of 24,000°K and below, only first ionization of air particles will be considered here. Unlike molecular dissociation, the internal energy of the ionized gas

is a sum of the thermal energy of its particles (atoms, ions, and electrons) and the energy required to remove electrons from the atoms and ions. The internal energy of a partially ionized gas, therefore, will be the energy of the ionized and unionized gas particles.

To examine the behavior of thermodynamic properties of air with temperature, three of its primary properties, i.e., the dimensionless internal energy (e/R T), enthralpy (h/R T), and the adiabatic exponent (γ), were obtained from the data given in Reference 13. These parameters were obtained between a temperature range of 300 and 24,000°K. A tabulation of the data at two different densities, namely, at the standard air density (ρ_o = 0.001293 gm/cm^3) and at 1/10 of the standard density, is given in Table 1. The variation of the parameters e/R T and h/R T with temperature is shown by the curves of Figure 5. The temperature lines at which the contributions by various degrees of freedom become accountable are clearly marked on the curves. It is obvious from Table 1 and from the curves that the energy functions e/R T and h/R T undergo a wide variation as the air temperature increases from 300 to 24,000°K. Correspondingly, the adiabatic exponent, γ, goes through a wide variation from the classical value of 1.4 at 300°K to around 1.15 at 10,000°K. Figure 6 shows plots of γ versus temperature at the two selected air densities.

Table 1. Thermodynamic Properties of Air (After Reference 13)

Temperature, T (°K)	Thermodynamic Properties[a]					
	At Standard Density, ρ_o[b]			At 1/10 of Standard Density, ρ_o		
	e/R T	h/R T	γ	e/R T	h/R T	γ
300	2.5	3.5	1.4	2.5	3.5	1.4000
1,000	2.630	3.63	1.38	2.63	3.63	1.3800
2,000	2.962	3.963	1.3378	2.966	3.967	1.3375
3,000	3.395	4.402	1.2967	3.677	4.699	1.2780
4,000	4.345	5.408	1.2447	5.311	6.445	1.2135
5,000	5.138	6.283	1.2290	5.746	6.945	1.2087
6,000	5.502	6.700	1.2178	6.517	7.784	1.1944
7,000	6.623	7.533	1.2028	8.732	10.163	1.1639
8,000	7.744	9.144	1.1808	11.67	13.349	1.1439
12,000	12.18	14.139	1.1608	13.47	15.531	1.1530
18,000	13.04	15.323	1.1751	18.13	20.906	1.1531
24,000	16.09	18.96	1.1781	21.83	25.432	1.1650

[a] e is the specific internal energy, and h is the specific enthalpy of air.
The adiabatic exponent γ = h/e.

[b] $\rho_o = 1.293 \times 10^{-3}$ gm/cm^3.

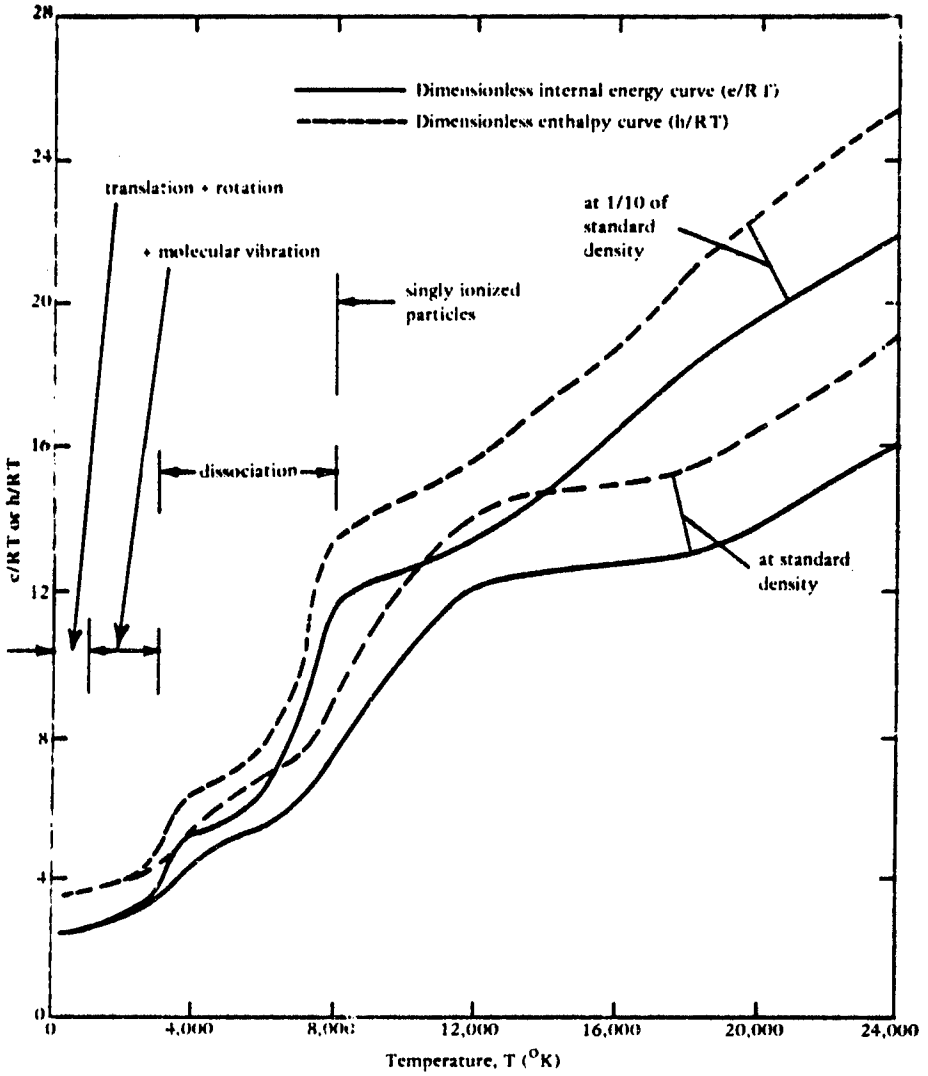

Figure 5. Variation of internal energy and enthalpy with temperature for air.

In the light of the foregoing discussion it is concluded that the perfect gas equation given in Equation 39 must be modified for computing the shock flow parameters through high temperature air. One such modification commonly used is given by [12-15]

$$p = Z(p,T)\,\frac{RT}{V} \tag{40}$$

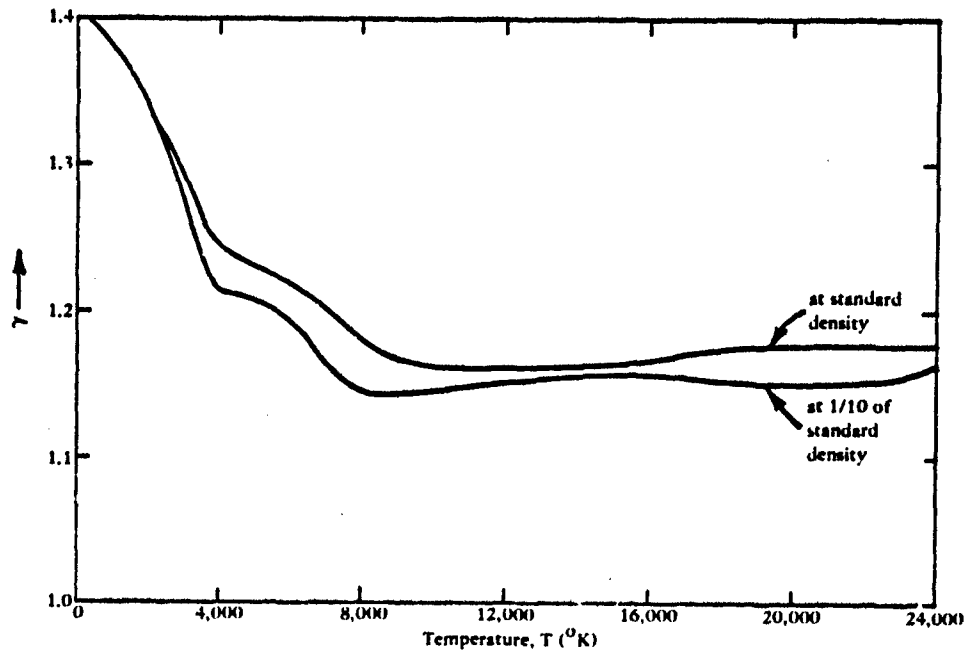

Figure 6. Variation of the adiabatic exponent with temperature for air.

where $$Z(p,T) = f(\alpha, \alpha^1) \quad (41)$$

α is the degree of molecular dissociation, and α^1 is the degree of particle ionization. The quantity Z, commonly known as the "compressibility factor," is a function of pressure and temperature of the gas. At temperatures of 1,000°K or less and moderate pressures the perfect gas equation gives satisfactory results. Thus, Z = 1.0 at these temperatures and pressures, yielding the perfect gas equation. The quantity Z for air at a given temperature and density is found from standard tables given in References 13 and 15. These are included as Table 2 for easy reference.

The Rankine-Hugoniot Relationships for High Temperature Shock Waves. When moderately high overpressures and high temperature shocks propagate through cold air, the thermodynamic properties, such as the internal energy function (e/R T), the enthalpy function (h/R T), and the adiabatic exponent (γ = h/e), vary nonuniformly with temperature (Figures 5 and 6). The nonuniform variation, as discussed earlier, is attributed mainly to molecular dissociation and particle ionization. Thus, the Rankine-Hugoniot relationships, because of their dependence upon the above parameters, change in a nonuniform manner. Therefore, it is not possible to define simple analytical expressions describing the pressure, density, and temperature ratios across the shock. There are some iterative procedures, which are based upon the tabulated value of the compressibility factor Z and the adiabatic exponent γ, which render semi-analytical expressions for the shock wave parameters [12, 13, 14].

Gilmore [13] plots the density and temperature ratios (ρ_2/ρ_1 and T_2/T_1) across the shock in the standard Hugoniot form, i.e., against the pressure ratio (P_2/P_1) for density values behind the shock ρ_2 of 10, 1, 10^{-1}, 10^{-2}, 10^{-3}, and 10^{-4} of the standard air density ρ_0 = 0.001293 gm/cm^3. Gilmore in his plots defined suffix 1 to refer to the quantities ahead of the shock, and suffix 2 was used for quantities behind the shock.

The plots are based upon a normal shock wave propagating into cold air at a temperature T_1 of 273.2°K. The plots also show the variation of the Mach number of shock as

$$\frac{u_s}{c_1} = \sqrt{\frac{(\rho_2/\rho_1)(p_2/p_1 - 1)}{\gamma_1(\rho_2/\rho_1 - 1)}} \tag{42}$$

with the pressure ratio p_2/p_1. The quantity u_s is the speed of the shock, and c_1 is the speed of sound in the cold air. These Rankine-Hugoniot plots, which include the real gas effects, are given in Figure 7 for normal shocks traveling through air at a density of 0.001293 gm/cm^3.

Computations Using the Real Gas Equation of State. The Lagrange computer program has an equation of state algorithm built into it. The algorithm based upon a value of the internal energy, e, and the air density, ρ, computes the adiabatic exponent, γ, from the tabulated values of Gilmore [13]. From known values of e, ρ, and γ the value for the pressure is computed using the relationship

$$p = \rho e(\gamma - 1) \tag{43}$$

From the known value of p, the algorithm refines the previously calculated values of e and ρ for further computing.

The algorithm has a built in numerical routine to obtain a correct value of air temperature. The method is based upon computing the air temperature from known p and ρ using Equation 40. Since the quantity Z is a function of pressure p and temperature T, calculation of temperature using Equation 40 is, therefore, an iterative process. The numerical routine performs the required iteration accurately, using the tabulated values (Table 2) of Z given by Gilmore [13].

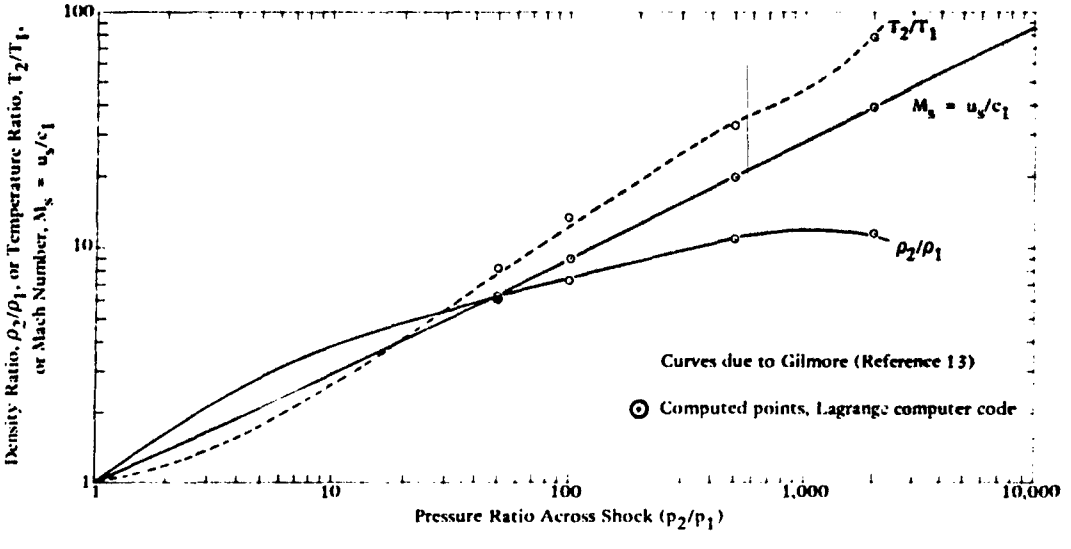

Figure 7. Rankine-Hugoniot curves including real gas effects for shock waves in air.

Table 2. Values of the Compressibility Factor Z(p,T) (After Reference 13)

Temperature, T (^{o}K)	Compressibility Factor for Density Ratio, ρ/ρ_0, of—							
	10	10^{0}	10^{-1}	10^{-2}	10^{-3}	10^{-4}	10^{-5}	10^{-6}
1,000	1.0000	1.0000	1.0000	1.0000	1.0000	1.0000	1.0000	1.0000
2,000	1.0000	1.0000	1.0001	1.0007	1.0017	1.0055	1.0170	1.0487
3,000	1.0023	1.0072	1.0218	1.0610	1.1341	1.1912	1.2069	1.2109
4,000	1.0226	1.0628	1.1341	1.1896	1.2107	1.2282	1.2715	1.3883
5,000	1.0728	1.1448	1.1990	1.2370	1.3081	1.4835	1.7752	1.9544
6,000	1.1275	1.1984	1.2669	1.4001	1.6643	1.9143	1.9864	2.0051
7,000	1.1761	1.2699	1.4315	1.7162	1.9384	1.9970	2.0288	2.1105
8,000	1.2390	1.4001	1.6794	1.9259	2.0010	2.0487	2.1702	2.5007
12,000	1.708	1.957	2.062	2.224	2.636	3.365	3.865	3.968
18,000	2.063	2.284	2.775	3.518	3.910	3.984	4.078	4.530
24,000	2.322	2.865	3.602	3.930	4.143	4.778	5.623	5.931

Test Calculations. To check the accuracy of the algorithm, four trial runs, using the Lagrange computer program, for shocks traveling into still air at standard density and temperature through a straight duct were carried out at pressure ratios of 50:55, 101:77, 502:45, and 2008:8 across the shock. The computed shock Mach number, M_s, and the density and temperature ratios, ρ_2/ρ_1 and T_2/T_1, across the shock are given in Table 3. These values are also plotted on the Rankine-Hugoniot curves of Figure 7 for comparison with Gilmore's accurate values. It can be seen from Figure 7 that the shock parameters, namely the Mach number, and the density and temperature ratios across it are computed with good accuracy by the Lagrange computer program. For completeness, the values of the adiabatic exponent γ and the compressibility factor Z are also listed in Table 3.

Table 3. Shock Parameters Computed Using the Real Gas Equation of State[a]

Pressure Behind Shock, p_2 (psia)	Pressure Ratio, p_2/p_1	Shock Mach Number, $M_s = u_s/c_1$	Density Behind Shock, ρ_2 (gm/cm^3)	Density Ratio, ρ_2/ρ_1	Temperature Behind Shock, T_2 (^{o}K)	Temperature Ratio, T_2/T_1	Adiabatic Exponent, γ	Compressibility Factor, Z
743.1	50.55	6.34	7.447×10^{-3}	6.079	2,399	8.32	1.33	1.00
1,496.0	101.77	9.12	9.051×10^{-3}	7.389	3,876	13.45	1.28	1.02
7,386.0	502.45	19.94	1.341×10^{-2}	10.95	9,351	32.45	1.19	1.41
29,530.0	2,008.8	39.95	1.399×10^{-2}	11.42	22,470	77.97	1.19	2.26

[a] Pressure (p_1), temperature (T_1), and density (ρ_1) for the undisturbed air are taken as 14.7 psia, 288.2^{o}K, and 1.225×10^{-3} gm/cm^3, respectively.

EULERIAN COMPUTER CODE DESCRIPTION

The Basic Equations

The Eulerian code computes the flow variables in a duct through which a normal shock wave is passing. The flow variables are computed as functions of time and position. The shock wave is considered to be transmitted into the duct by a blast wave passing over the duct entrance. The computer code allows the shock wave to traverse the duct, be reflected from the closed end of the duct, and then re-traverse the duct in the opposite direction.

The conservation equations are written in the vector form.

$$\frac{\partial U}{\partial t} + \frac{\partial F(U)}{\partial x} + G(U) = 0 \tag{44}$$

where vectors U, F(U), and G(U) are given by

$$U = \begin{bmatrix} N \\ M \\ E \end{bmatrix} \tag{45a}$$

$$F(U) = \begin{bmatrix} M \\ \left(\frac{M^2}{N} + pA\right) \\ (E + p)\frac{M}{N} \end{bmatrix} \tag{45b}$$

$$G(U) = \begin{bmatrix} 0 \\ \left(fA\frac{\rho u^2}{8H} - p\frac{dA}{dx}\right) \\ \frac{Eu}{A}\left(\frac{dA}{dx}\right) \end{bmatrix} \tag{45c}$$

The quantities M, N, and E are defined as follows:

$M = \rho u A$

$N = \rho A$

$E = \rho(e + 1/2\, u^2)$

t = time

x = axial distance

ρ = density

e = internal energy per unit mass

p = pressure

$= p(e,\rho)$

$= \rho e(\gamma - 1)$, for a polytropic gas

f = wall friction coefficient

$= 4\tau_w/(1/2\,\rho\,u^2)$

u = velocity

τ_w = shear stress at duct wall

A = duct cross-sectional area

H = duct hydraulic radius

Substitution of the vectors U, F(U), and G(U) into Equation 44 yields the equations for the conservation of mass, momentum, and energy. The gas in the duct is considered to be inviscid (except at the duct wall) and thermally nonconducting. Pressure, density, and internal energy are related through the perfect gas equation of state.

Because the flow in the duct is time dependent, steady-state values of the wall friction coefficient, f, cannot properly be used. In the Eulerian code, the wall friction coefficient is computed from

$$f = S1\,(R_e)^{S2} \tag{46}$$

where R_e is the Reynolds number, based on duct equivalent diameter, and S1 and S2 are empirical constants.

The Finite-Difference Equations

A two-step integration technique, that of Lax and Wendroff (Reference 2), is used to solve the conservation equations, Equations 44 and 45. Referring to the sketch below, all the properties at time step n are known. The properties at time step n+1 and location j are to be computed.

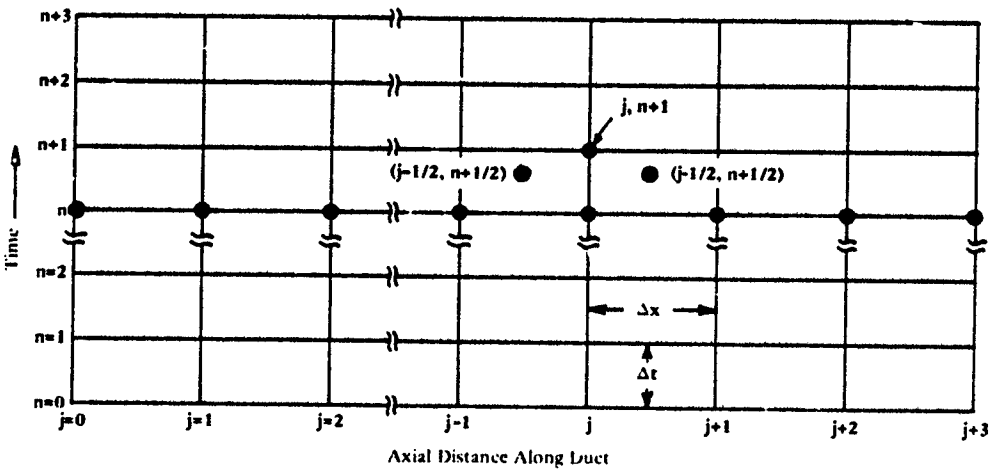

First, the properties at two intermediate steps (j-1/2, n+1/2) and (j+1/2, n+1/2) are computed from:

$$U_{j+1/2}^{n+1/2} = \frac{1}{2}\left(U_{j+1}^{n} + U_{j}^{n}\right) - \frac{1}{2}\left(\frac{\Delta t}{\Delta x} + g_2^{+}\right)\left(F_{j+1}^{n} - F_{j}^{n}\right)$$

$$- \frac{1}{2} g_1^{+}\left(U_{j+1}^{n} - U_{j}^{n}\right) + \frac{\Delta t}{4}\left(G_{j+1}^{n} + G_{j}^{n}\right) \qquad (47a)$$

$$U_{j-1/2}^{n+1/2} = \frac{1}{2}\left(U_{j-1}^{n} + U_{j}^{n}\right) - \frac{1}{2}\left(\frac{\Delta t}{\Delta x} + g_2^{-}\right)\left(F_{j}^{n} - F_{j-1}^{n}\right)$$

$$- \frac{1}{2} g_1^{-}\left(U_{j}^{n} - U_{j-1}^{n}\right) + \frac{\Delta t}{4}\left(G_{j-1}^{n} + G_{j}^{n}\right) \qquad (47b)$$

where F_j, G_j, etc., denote $F(U_j)$, $G(U_j)$, etc., and g_1^{+}, g_1^{-}, g_2^{+}, g_2^{-} are pseudo-viscosity factors, defined in Equation 49. With the properties at the two intermediate steps known, the properties at the new step (j, n+1) are computed from

$$U_{j}^{n+1} = U_{j}^{n} - \frac{\Delta t}{\Delta x}\left(F_{j+1/2}^{n+1/2} - F_{j-1/2}^{n+1/2}\right)$$

$$+ \frac{1}{2}\left(\frac{\Delta t}{\Delta x}\right) g_0^{+}\left(U_{j+1}^{n} - U_{j}^{n}\right) - g_0^{-}\left(U_{j}^{n} - U_{j-1}^{n}\right)$$

$$+ \frac{\Delta t}{2}\left(G_{j+1/2}^{n+1/2} + G_{n-1/2}^{n+1/2}\right) \qquad (48)$$

where g_0^{+} and g_0^{-} are pseudo-viscosity factors, defined in Equation 49. The pseudo-viscosity factors were obtained following the generalized procedure of Reference 4. This procedure yielded the following equations:

$$g_0^{+} = \alpha_1\left[\left(U_{j+1/2}^{n}\right)^2 - \left(c_{j+1/2}^{n}\right)^2\right] + \alpha_2 U_{j+1/2}^{n}\left(U_{j+1/2}^{n} - c_{j+1/2}^{n}\right)$$

$$+ \alpha_3 U_{j+1/2}^{n}\left(U_{j+1/2}^{n} + c_{j+1/2}^{n}\right) \qquad (49a)$$

$$g_1^{+} = -\left[2\alpha_1 U_{j+1/2}^{n} + \alpha_2\left(2U_{j+1/2}^{n} - c_{j+1/2}^{n}\right) + \alpha_3\left(2U_{j+1/2}^{n} + c_{j+1/2}^{n}\right)\right] \qquad (49b)$$

$$g_2^{+} = \alpha_1 + \alpha_2 + \alpha_3 \qquad (49c)$$

where

$$\alpha_1 = -\frac{1}{2} K_1 \frac{\left|U_{j+1}^{n} - U_{j}^{n}\right|}{\left(c_{j+1/2}^{n}\right)^2} \qquad (50a)$$

$$\alpha_2 = \frac{1}{4} K_2 \frac{\left|\left(U_{j+1}^{n} - U_{j}^{n}\right) + \left(c_{j+1}^{n} - c_{j}^{n}\right)\right|}{\left(c_{j+1/2}^{n}\right)^2} \qquad (50b)$$

$$\alpha_3 = \frac{1}{4} K_3 \frac{\left|\left(U^n_{j+1} - U^n_j\right) - \left(c^n_{j+1} - c^n_j\right)\right|}{\left(c^n_{j+1/2}\right)^2} \tag{50c}$$

and c = acoustic velocity.

Values of K_1, K_2, and K_3 of 2.0 have been empirically found to be of the proper magnitude. The expressions for $\bar{g_0}$, $\bar{g_1}$, and $\bar{g_2}$ are obtained by replacing j by j-1 in Equations 49 and 50.

The stability requirement for selecting the time step is:

$$\Delta t = \frac{\Delta x}{F(u + c)} \tag{51}$$

where F is a factor greater than unity. Numerical results have shown that too small a time step results in oscillatory solutions. Thus, the value of F should be the smallest value (>1) that will yield a stable solution. The optimum value for F was found to be 1.5. In the computer code, the time step Δt is recomputed for each cycle, using the minimum value of $|u| + c$ of the preceding cycle.

The Boundary Conditions

The pressure at the entrance of the duct is specified as a function of time in the same manner as in the Lagrange Code (Equation 10):

$$p(0,t) = p_a + [p(0,0) - p_a]\, e^{-t/t_i} \tag{52}$$

where p(0,t) = pressure at x = 0, t = t. The initial pressure at the duct entrance, p(0,0), is computed (as in the Lagrange Code, Equation 18) from:

$$p(0,0) = p_a + 0.969(p_s - p_a)^{0.804} \tag{53}$$

With p(0,t) known, the density $\rho(0,t)$ is computed from the isentropic relationship

$$\rho(0,t) = \rho(0,0)\left[\frac{p(0,t)}{p(0,0)}\right]^{1/\gamma} \tag{54}$$

where γ is the ratio of specific heats, considered constant in this study.

The initial value of density $\rho(0,0)$ is computed from the Rankine-Hugoniot relationship

$$\rho(0,0) = \rho_a \left[\frac{(\gamma + 1)\frac{p(0,0)}{p_a} + (\gamma - 1)}{(\gamma - 1)\frac{p(0,0)}{p_a} + (\gamma + 1)}\right] \tag{55}$$

where ρ_a is the ambient value of density. Internal energy e is computed from the equation of state (Equation 43), written in the form

$$e(0,t) = \frac{p(0,t)}{\rho(0,t)(\gamma - 1)} \tag{56}$$

The initial velocity $u(0,0)$ is computed from the moving normal shock relationship

$$u(0,0) = u_s\left[1 - \frac{\rho_a}{\rho(0,0)}\right] \tag{57}$$

where u_s, the velocity of the normal shock wave, is computed from

$$u_s = c_0\left[\frac{\frac{p(0,0)}{p_a}(\gamma+1) + (\gamma-1)}{2\gamma}\right] \tag{58}$$

where c_0 is the ambient acoustic velocity. Because a rational basis for specifying $u(0,t)$ a priori is not known to the authors, the expediency of setting $u(0,t)$ equal to $u(\Delta x,t)$ was employed, where Δx is the numerical increment of x used in the numerical solution of the conservation equations.

At the end of the duct, $x = L$; the rigid wall boundary condition can be imposed as $u(L,t) = 0$. Within the framework of the numerical integration scheme, this was accomplished by means of a virtual station beyond the end of the duct, located at $L + \Delta x$. By setting $u(L+\Delta x,t)$ equal to $-u(L-\Delta x,t)$, the proper boundary condition at $x = L$ was obtained.

NUMERICAL RESULTS

Lagrange Computer Code

The results from the Lagrange computer code are presented in Reference 1 for the particular case of a constant area duct. A summary of these results is reproduced in Figures 8 and 9, in which computed data are compared with the shock tube experimental data of Reference 6. These comparisons show the degree of accuracy of the computer code when a constant friction factor is used and demonstrate the effect of wall friction on shock wave attenuation.

Computed results, which include the variable area option, are presented in Figure 10. Shock wave pressure change through a duct cross-sectional area increase is given for outlet-to-inlet-area ratios up to 10. The analytical curve is compared with Stanford Research Institute shock tube experimental data [16] and with data from the 500-ton TNT blast experiments of EVENT DIAL PACK [5]. The duct diameter at the inlet to the area change was 2 inches in the SRI experiments and 24 inches in the DIAL PACK experiments. The comparison demonstrates the adequacy of the computer code to predict shock strength change with duct area increase.

Pressure-versus-time waveforms are presented in Figure 11 for the Lagrange Code solution with a comparison to results from the Eulerian Code (discussed in a following section). The reflected wave at the closed end of the duct is also shown in the figure. The overpressure of this reflected wave is approximately 10% below the value estimated by Rankine-Hugoniot relationships. Studies have shown, however, that the incident wave and reflected wave overpressures at a rigid boundary computed for a shock wave of constant strength by the Lagrange Code agrees well with Rankine-Hugoniot values; this implies a small reflected wave inaccuracy for waves with rarefaction behind the shock.

The computed results using the Lagrange Code for the case of a 1-Mt nuclear surface wave are given in Figure 12. The air entrainment system is a typical configuration except for possible variations in the scale. The location of the inlet was selected as 1,500 feet from the center of the nuclear burst. The required surface wave parameters were obtained from Reference 7. The pressure and temperature values shown in the figure depict the state of the air in the system at a time of 0.0108 second after arrival of the nuclear wave at the inlet. The

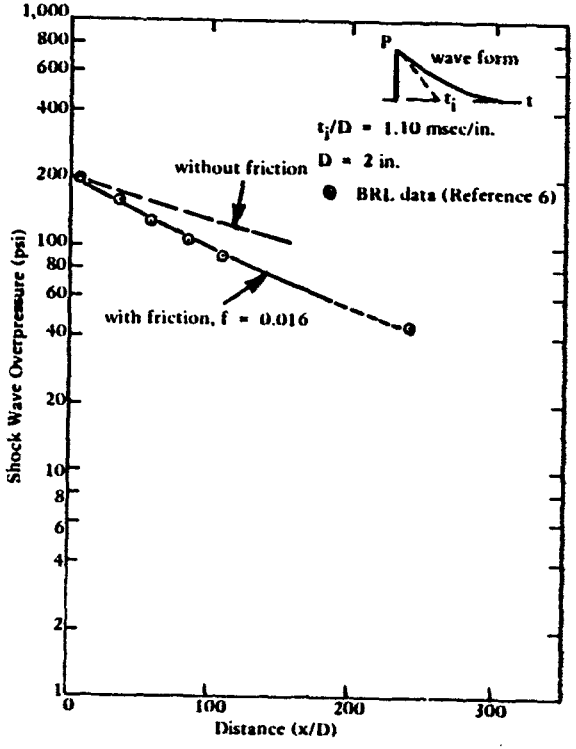

Figure 8. Effect of wall friction on prediction of shock wave attenuation.

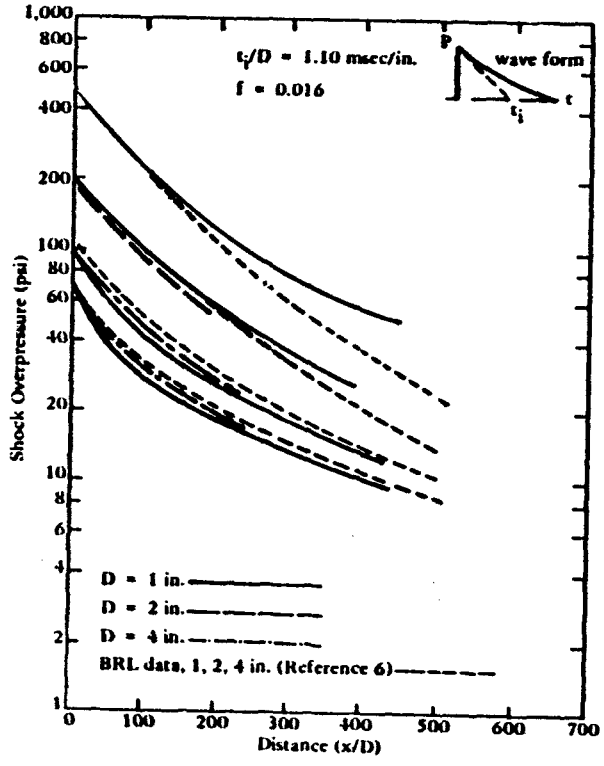

Figure 9. Shock wave attenuation—computed results compared with data.

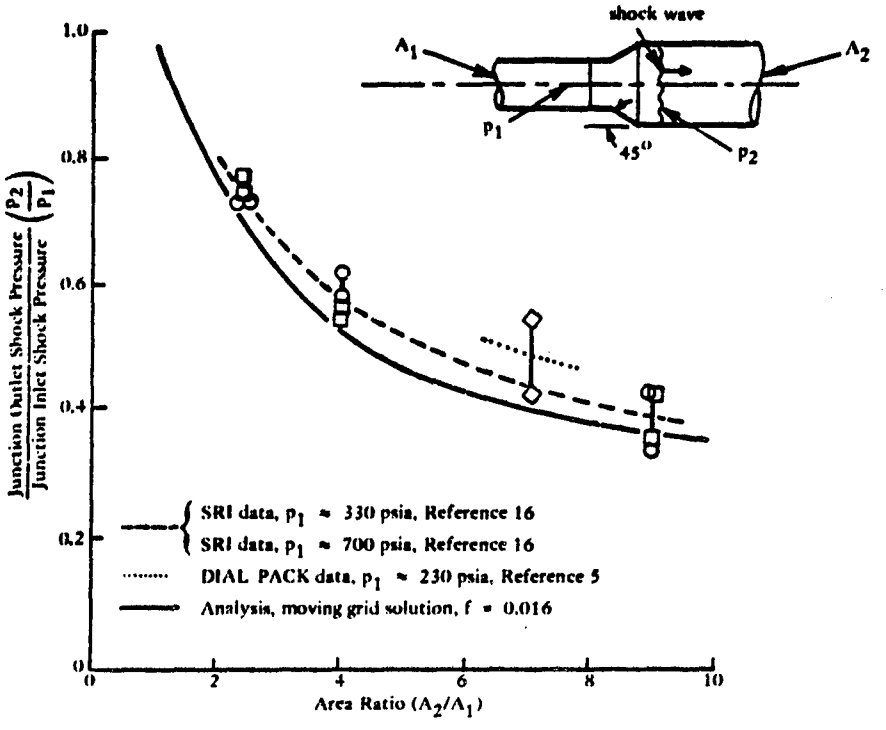

Figure 10. Effect of area change on shock pressure.

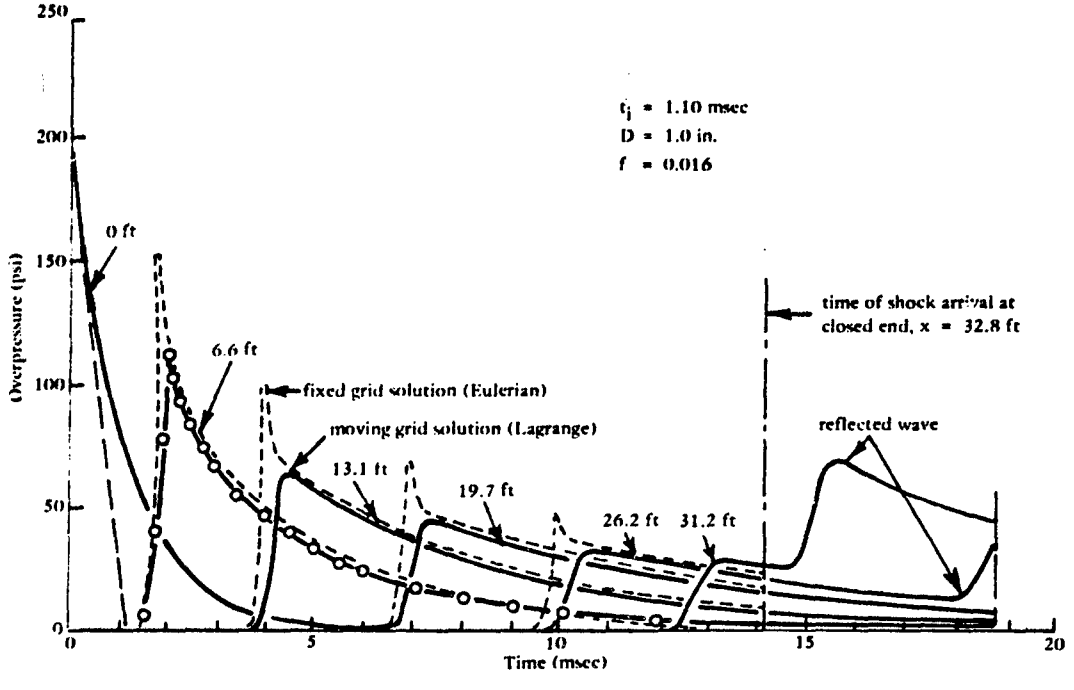

Figure 11. Pressure-time wave forms.

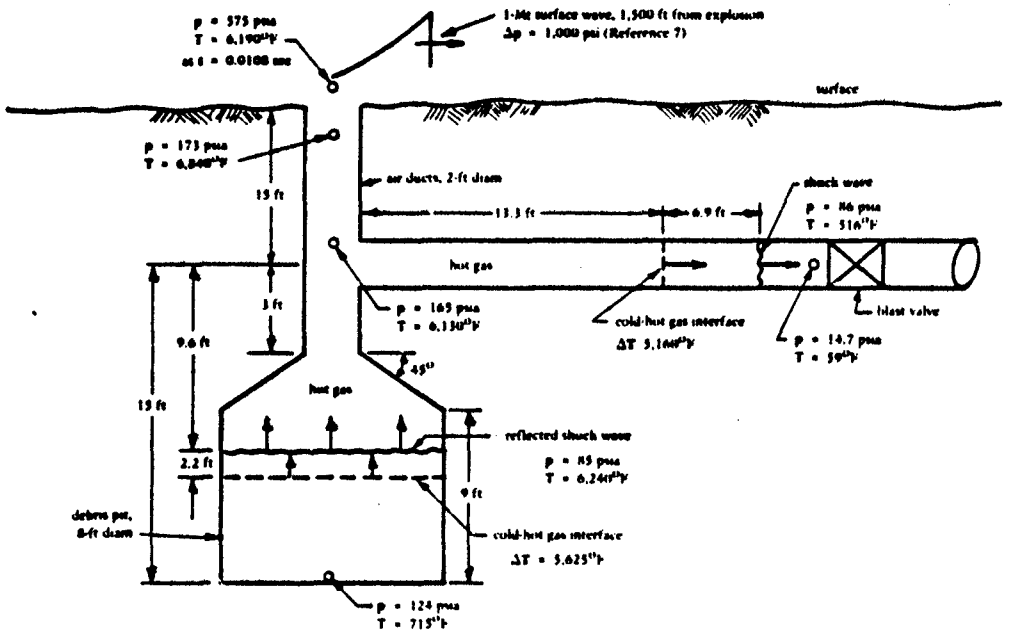

Figure 12. Typical computed results—Lagrange code, 0.0108 second after arrival of shock wave from 1-Mt nuclear explosion.

shock wave and cold-hot gas interface (contact surface) locations are shown as a line boundary. The computer program, however, spreads the shock wave over approximately five finite-difference grid mesh lengths, due to the pseudo-viscosity technique used, and spreads the contact surface also over approximately five mesh lengths. The shocks are accurately located through utilization of the maximum value of the pseudo-viscosity parameter, and this is the location shown. The contact surface location shown is the location of the zone interface across which the leading downstream temperature jump occurs and is the location were the total temperature jump will occur (neglecting diffusion effects) in the actual case. Figure 12 is an example of the computer predictions at a particular time and not the complete results of the computer output. For example, for this calculation the time history of all parameters was available at several locations in the system. These time histories are not shown because they would not add significantly in presenting a sample calculation. The computer code complete output capabilities are explained in Appendix A.

When a reflected shock wave reaches the T-junction (Figure 12), the computer program terminates computation because the T-junction programming will not allow reversal of the direction of the inlet or exit velocities at this junction. This fact, however, does not seriously limit the capabilities of the computer code. As examination of Table 4 shows, the area expansion ratio for the debris pit inlet has negligible effect on the flow parameters in the inlet duct and in the duct to the blast valve. Therefore, any given problem can be calculated in two steps as follows: step 1, calculate the inlet duct and debris pit flows using the configuration shown in Figure 1b; step 2, calculate the blast valve duct flow by using the configuration shown in Figure 2 with the debris pit duct and debris pit replaced by a constant area duct. This constant area duct should be

sufficiently long to allow the reflected wave in the blast valve duct to reach the T-junction prior to the time when a reflected wave in the constant area duct would reach the T-junction. This allows sufficient completion of the primary shock propagation problem in the blast valve duct. The debris pit solution (step 1), however, will be conservative since the pressure loss through the T-junction, which is approximately 20%, will not be included. Neglected in the above procedure is the interaction of primary and reflected shock waves, e.g., the effects of a reflected wave from the debris pit propagating into and down the blast valve duct. Computation of shock wave interaction is not considered important since flow reversal will have taken place in all ducts prior to any shock interactions for the configuration of concern, and solution of the primary problem will have been completed.

Table 4. Effect of Area Expansion Ratio of Debris Pit on Inlet Duct Flow and Blast Valve Duct Flow[a]

Area Expansion Ratio	Shock Propagation Time[b] (sec)	Parameters at Exit to Inlet Duct			Shock Parameters in Blast Valve Duct				Interface Parameters in Blast Valve Duct	
		p (psia)	T (^{O}K)	u (cm/sec x 10^{-4})	p (psia)	T (^{O}K)	u (cm/sec x 10^{-4})	x (cm)	ΔT (^{O}K)	x (cm)
1.0	0.00880	247	3,693	8.27	82.6	546	5.05	480	2,964	317
5.0	0.00867	249	3,693	8.44	81.3	553	4.98	458	2,956	310
10.0	0.00842	256	3,692	8.44	81.3	545	4.99	448	2,937	295
16.0	0.00881	234	3,664	8.75	80.9	543	5.01	480	2,747	319

[a] Configuration of Figure 2 with 1-Mt nuclear surface wave at 1,500-foot radius.
[b] Number of computation cycles was 1,000 for all cases.

Eulerian Computer Code Results

The Eulerian Code results are given for a constant area duct only. The variable area option for this code is not accurate and should not be used. For variable area problems the Lagrange Code is more appropriate. Since the Lagrange Code was in agreement with experimental data, the output of the Eulerian Code was compared to the Lagrange Code results to verify the Eulerian Code accuracy. This comparison is presented in Figure 14. The time waveforms for overpressures are given at four locations in a duct through which an attenuating shock wave is propagating. The Eulerian solution agrees well with the Lagrange solution except for an overshoot at the shock front. This overshoot is characteristic of the Lax-Wendroff finite-difference scheme that is used [2]. The shock front is steeper in the Eulerian solution, and the shock speed is somewhat faster than in the Lagrange solution. This difference in shock speed is attributed to the pressure overshoot which affects shock front attenuation due to rarefaction decay.

Studies concerned with reflected shock waves at a rigid boundary show the reflected wave to have the characteristic overshoot. But the reflected pressure after the overshoot agrees with Rankine-Hugoniot relationship predictions.

A description of the input and output parameters that are used in the Eulerian Code with information on obtaining a Code listing is given in Appendix B.

CONCLUSIONS AND RECOMMENDATIONS

Both the Lagrange computer code and the Eulerian computer code presented are shown to be adequate for predicting shock wave propagation in a constant area duct. For shock wave prediction in a variable area duct the Lagrange Code should be used. Both codes adequately predict shock wave reflection from a rigid boundary and are suitable for either constant strength shock waves or shock waves with a rarefaction region with exponential pressure decay behind the shock front. For shock wave prediction in an air entrainment system consisting of debris pit and blast valve ducts (Figure 2) the Lagrange computer code should be used, in which case the simulated surface wave can be of Hiroshima nuclear explosion or TNT explosion origin.

ACKNOWLEDGMENTS

The very difficult computer programming required to develop the Lagrange computer code was done by Mrs. Rita Brooks of CEL.

REFERENCES

1. Naval Civil Engineering Laboratory. Technical Note N-1205: Shock wave propagation through air entrainment systems–Phase I, by R. H. Fashbaugh and A. Widawsky. Port Hueneme, CA., Feb 1972.

2. R. D. Richtmyer and K. W. Morton. Difference methods for initial-value problems, 2nd ed., New York, Interscience Publishers, 1957, pp 288-388.

3. New York University. Report NYO-1480-33: Finite difference calculations for hydrodynamic flows containing discontinuities, by S. Z. Burstein. Sep 1965.

4. S. Z. Burstein. "Numerical methods in multidimensional shocked flows," A.I.A.A. Journal, Vol. 2, No. 12, Dec 1964, pp 2111-2117.

5. Naval Civil Engineering Laboratory. Technical Note N-1181: High explosive field test of a hardened air entrainment system, by D. E. Williams and R. H. Fashbaugh. Port Hueneme, CA., Oct 1971.

6. Ballistic Research Laboratories. Memorandum Report No. 1809: Attenuation of peaked air shock waves in smooth tunnels, by G. A. Coulter. Aberdeen Proving Ground, MD, Nov 1966.

7. The Rand Corporation. Report No. R-425-PR: A review of nuclear explosion phenomena pertinent to protective construction, by H. L. Brode. Santa Monica, CA., May 1964.

8. Ballistic Research Laboratories. Memorandum Report No. 1390: Information summary of blast patterns in tunnels and chambers, by Shock Tube Facility Staff. Aberdeen Proving Ground, MD, Mar 1962.

9. A. W. Zimmerman. Flow through duct junctions of a hardened ventilation system due to a nuclear burst, TRW Systems. Redondo Beach, CA., R-11466-6055-R00-00, 1968.

10. C. A. Kot, et al. Air blast attenuation and applications to hardened power systems, IITRI. Chicago, IL., IITRI-J6014(2), 1969.

11. B. E. L. Deckker, and D. H. Mole. Fluid dynamic aspects of unsteady flow in branched ducts, Proc. Instn. Mech. Engrs., Vol. 182, Pt 3H, 1967-68, pp 167-174.

12. J. N. Bradley. Shock waves in chemistry and physics. New York, John Wiley and Sons, Inc., 1962.

13. The Rand Corporation. Research Memorandum RM-1543: Equilibrium composition and thermodynamic properties of air to 24,000°K, by F. R. Gilmore. Santa Monica, CA, 24 Aug 1955.

14. Ya. B. Zel'dovich and Yu. P. Raizer. Physics of shock waves and high-temperature hydrodynamic phenomena, Vol. 1, ed. by Wallace D. Hayes and Ronald F. Probstein. New York and London Academic Press, 1966, pp 176-215.

15. National Bureau of Standards. Report AEDC-TR-65-58: Tables of thermodynamic properties of air in chemical equilibrium including second virial corrections from 1,500°K to 15,000°K, by Joseph Hilsenrath and Max Klein. Washington, D.C., Mar 1965.

16. Stanford Research Institute. Report No. C-0096: Measurements of shock wave attenuation in various duct components–Phase II and III, by H. R. Bredfeldt and R. J. Kier. Menlo Park, CA., Jul 1968.

17. Naval Ordnance Laboratory. Report No. TR-62-168: One-dimensional hydrodynamic code for nuclear-explosion calculations, by D. Lehto and M. Lutsky. White Oak, Silver Spring, MD, Mar 1965.

18. University of California Lawrence Radiation Laboratory. Report No. UCRL-6919: A computer program for calculating one-dimensional hydrodynamic flow–KQ CODE, by M. Wilkins et al. Livermore, CA., Apr 1963.

Appendix A

LAGRANGE COMPUTER CODE DESCRIPTION

INTRODUCTION

The Lagrange computer code is similar in basic structure to the WUNDY code reported in Reference 17, which was based on the KO-CODE of the University of California Radiation Laboratory [18]. The basic structure of the Lagrange Code and the input and output formats are described below. The computer code listing and card deck can be obtained by requesting a program tape from the Computer Center, Code L06, CEL. All quantities in the code are given in cgs units except for printout of pressure which is given in psia.

CODE BASIC STRUCTURE

The computer code consists of a main control subroutine with several auxiliary subroutines. A list of these subroutines with a description of each function follows.

Subroutine	Function
MAIN	Controls main logical flow and reads input data
BDY1	Specifies motion of interface at duct inlet for low temperature wave
BDY123	Specifies motion of interfaces at T-junction
BDY2	Specifies motion of interface at a duct exit
DATEXP	Data source for duct inlet losses
EQST	Controls equation of state subroutine acquisition
EQS1	Equation of state for ideal gas ($T < 1{,}000^{o}K$)
EQS3	Equation of state for real air ($T < 24{,}000^{o}K$)
GENR	Initializes problem
GEOM	Calculates cross-sectional area and zone volume
HTEMP	Calculates Z for EQS3
HYDR	Computes hydrodynamic motions
NUBDY	Specifies motion of interface at duct inlet for 1-Mt nuclear wave case
OUT1	Prints normal output, pressure, etc., in each zone at fixed times
OUT2	Accumulates data on main shock front in each duct
OUT3	Accumulates pressure, etc., versus time at fixed positions
OUT4	Punches cards from which the problem can be continued
REZ1	Removes excessively compressed zones

Subroutine	Function
REZEN1	Adds a zone at duct entrance for mass inflow
REZEN	Controls entrance zone size at T-junction
REZEX1	Controls exit zone size at T-junction
TIMEST	Calculates time step

CODE INPUT QUANTITIES AND FORMATS

The input data symbols, including the data card number on which they appear, and the data format are given in Table A-1. The data appears on a particular card in the order in which it is given. A sample data card listing is given in Table A-2 for a 1,500-foot radius location from a 1-Mt nuclear burst with an air entrainment geometry as shown in Figure 12.

CODE OUTPUT VARIABLES AND FORMATS

The output of this computer code consists of printout of the input data, corrected input data, OUT1 subroutine printout, OUT2 subroutine printout, and OUT3 subroutine printout. The OUT4 subroutine punches cards. To give a full output would be too lengthy; therefore, only a sample output from printout of the input data and OUT1 at cycle 500 are given in Tables A-3 and A-4, respectively. The data in Tables A-2 through A-4 are for the problem of Figure 12. The program was run on a CDC 6600 computer, and it required a core storage of 165,000 and a running time of 119 seconds.

The normal output is provided by the OUT1 subroutine, which prints out the velocity, displacement, and several state variables for each zone at desired times. The printout is controlled by the quantity NPR. The variables printed out every NPR cycles of computation are given in Table A-5.

An auxiliary output is provided by the OUT3 subroutine, which prints out variables at desired locations in the duct versus time. The control variable $(I,J) specifies the location at which the variables given in Table A-6 are printed out.

Table A-1. Input Quantities

Card Number	Format	Symbol	Definition
1	7A10	ALIST(I)	Problem identification
2	7A10	ALIST(I)	Problem identification continued
3	1215	NPROB	Problem number
		IMAXL	Total number of ducts, 1 or 3
		INTAPE	≠ 0, no data input from tape 18
		INCODS	= 0, no extra input from cards

continued

Table A-1. Continued

Card Number	Format	Symbol	Definition
		NQUIT	Total number of cycles to run
		NPR	Print after every NPR cycle
		NTAPE	= 0, do not write tape 18
		KOPT	= 1, side-on type entrance
			= 0, wave originates at duct entrance
4	1215	KOUT2	= 0, do not call OUT2 (usually 4 when OUT2 is used)
		KOUT2A	Store data every KOUT2 cycles
		KOUT2B	Controls coupling between OUT2 and OUT3; usually zero
		KOUT3A	Store P-T data every KOUT3 cycles
		KOUT4	Punch continuation cards at KOUT4 cycles
		KREZ1	= 0, REZ1 not used
			= 1, REZ1 used
5	1215	NC(1) through NC(12)	Control variables, all zero except NC(6) and NC(7)
		NC(6)	= 1, print NC(6) times per decade in time
		NC(7)	= 1, use special pseudo-viscosity
6	1215	NC(13) through NC(24)	Control variables, all zero except NC(17)
		NC(17)	= 1, print GRAMS instead of PDYN
7	7E10.4	EBI	= 0, not now used
		T	= 0, start with time zero
		DTMIN(2)	= 0, use built-in time step
		DTRATE	= 0, use built-in time step change rate of 1.4
		STABIL	= 0, use built-in stability constant of 0.81
		UCUT	= 0, use built-in velocity cutoff value of 1×10^{-2} cm/sec

continued

Table A-1. Continued

Card Number	Format	Symbol	Definition
8	7E10.4	A1 through A5	Surface wave constants
9	7E10.4	B1 through B7	Surface wave exponents
10	7E10.4	DP	Positive pressure phase duration
		DU	Positive velocity phase duration
		TS	Shock arrival time
		TB	Time of maximum temperature
		PSO	Initial value, nuclear wave pressure
		QSO	Initial value, nuclear wave dynamic pressure
11	7E10.4	TMPS1	Surface temperature constant
		TMPS2	Surface temperature constant
		FLAG	= 1, use NUBDY subroutine
			= 0, use BDY1 subroutine
12	7E10.4	TLIST(1) through TLIST(6)	All zero, printing controlled by NPR
13	515	I = 1	Duct identification
		NEQST(1)	Number of equation of state in duct 1
		JCALC(1)	Number of last interface currently being calculated in duct 1
		NZONES(1)	Total number of zones in duct 1
		KOUT3(1)	Store P-T data at KOUT3 locations in duct 1
14	8E10.0	GAMMAI(1)	Gamma used in duct 1
		OUTBDY(1)	Length of duct 1
		EINIT(1)	Initial internal energy in duct 1
		UINIT(1)	Initial velocity in duct 1
		DINIT(1)	Initial density in duct 1

continued

Table A-1. Continued

Card Number	Format	Symbol	Definition
		FRICT(1)	Friction factor in duct 1
		CINQ(1)	2.0, pseudo-viscosity constant, duct 1
		AINQ(1)	0.2, pseudo-viscosity constant, duct 1
15	6E10.0	DO(1)	Diameter for X(I, J) < X1(1)
		D1(1)	Linear rate of change in diameter
		D2(1)	= 0, not used
		D3(1)	= 0, not used
		X1(1)	Begin linear diameter change at X1(1), duct 1
		X2(1)	End linear diameter change at X2(1), duct 1
16	6E10.0	S(1, 1) through S(1, 6)	Positions in duct 1 to collect P-T data by OUT3; zero if not used

Note: Repeat cards 13 through 16 for I = 2, IMAXL.

Last card	I5	NEXT	= 1, read new set of data
			≠ 1, stop; end of computation

Table A-2. Data Card Listing—Problem of Figure 12.

```
NUCLEAR HUMSI , SHOCK MS=20.7,    DIAM=2 FT,
ACEL, 09/17/73
 103     3     0     0   500    50     0     1
   1    10     0    10   500     1
   0     0     0     1     1     1     1     0     0     0     0     0     0
   0     0     0     1     1     0     0     0     0     0     0     0     0
0.     +00 0.     +00 0.     +00 1.     +00 0.     +00 0.     +00
1.5    +01 3.     +01 5.5    +01 3.2    +01 6.8    +01
2.9    +00 6.1    +01 1.3    +02 1.5    +02 3.5    +02 2.197 +00 0.     +00
1.2    +00 2.5    +00 H.     +02 2.7    +01 6.89   +07 2.     +0A
2.A    +03 3.     +04 1.     +30
0.     +00 0.     +00 0.     +00 0.     +00 0.     +00 0.     +00
   1     3     5    15     2
1.4    +00 4.5    +02 2.1A8  +19 0.     +00 1.225  -03 1.6    -02 2.    +00 2.    -01
6.     +01 0.     +00 0.     +00 0.     +00 0.     +00 0.     +00
4.4    +01 4.05   +02 0.     +00
   2     3     5    30     3
1.4    +00 4.5    +02 2.1A8  +19 0.     +00 1.225  -03 1.6    -02 2.    +00 2.    -01
6.     +01 2.     +00 0.     +00 0.     +00 0.     +01 1.8    +02
3.     +01 2.1    +02 4.2    +02
   3     3     5    51     2
1.4    +00 1.5    +03 2.1A8  +19 0.     +00 1.225  -03 1.6    -02 2.    +00 2.    -01
6.     +01 0.     +00 0.     +00 0.     +00 0.     +00 0.     +00
4.4    +01 6.     +02 0.     +00
   0
```

Table A-3. Printout of Input Data Problem of Figure 12.

```
 PRINTOUT OF INITIAL CONSTANTS

NUCLEAR BURST , SHOCK HEIGHT,    DIAMETER FT.
NCFL=  09/17/73

 NPROB     IMAX   IATAPE   IACCNS   NOUIT     NPR    NTAPE    NOPT
   123        3        0        2     500      50        9       1

 NOUT1   NOUT2A   NOUT2B   NOUT3A   NOUT4   NAP21
     1       10        0       10     500       1

 NC(1)   NC(2)   NC(3)   NC(4)   NC(5)   NC(6)   NC(7)   NC(8)   NC(9)  NC(10)  NC(11)  NC(12)
     0       0       0       1       1       1       1       0       0       0       0       0

NP(13)  NC(14)  NC(15)  NC(16)  NC(17)  NC(18)  NC(19)  NC(20)  NC(21)  NC(22)  NC(23)  NC(24)
     0       3       0       1       1       0       0       0       0       0       0       0

EPI                T                DTMIN(2)           DTRATE             STABIL              UCUT
  0.                0.                0.                 0.                 0.                 0.

  A1                A2                A3                 A4                 A5
  1.500000E-01       3.000000E-01       5.000000E-01       3.250000E-01       4.000000E-01

  B1                B2                B3                 B4                 B5                 B6                 B7
  2.000000E+00       2.100000E+01       1.300000E+02       1.500000E+02       3.500000E+02       2.197000E+00       0.

  DP                DU                TS                 TM                 PS0                QS0
  1.200000E+04       2.500000E+00       0.000000E+02       2.700000E+01       4.000000E+07       2.000000E+00

        TMPS1              TMPS2              FLAR
  2.000000E+03       3.000000E+00       1.000000E+00

                    TLIST
  0.                0.                0.                 0.                 0.                 0.

    I   NPOST   JCALC   NZONES   NOUTP
    1       3       0       15       2
    2       3       4       70       1
    3       3       5       94       2

        GAMMA1          OUTROV          EINIT           UINIT           DINIT           FRICT           CINQ            AINQ
    1  1.400000E+00    4.500000E+02    2.000000E+09    0.              1.225000E-03    1.000000E-02    2.000000E+00    2.000000E-01
    2  1.400000E+00    4.500000E+02    2.000000E+09    0.              1.225000E-03    1.000000E-02    2.000000E+00    2.000000E-01
    3  1.400000E+00    1.500000E+03    2.000000E+09    0.              1.225000E-03    1.000000E-02    2.000000E+00    2.000000E-01

        D0              D1              P2              P3              X1              X2
    1  0.000000E+01    0.              0.              0.              0.              0.
    2  0.000000E+01    2.000000E+00    0.              0.              9.000000E+01    1.000000E+02
    3  0.000000E+01    0.              0.              0.              0.              0.

                S
    1  4.500000E+01    4.050000E+02    0.              -0.             -0.             -0.
    2  3.000000E+01    2.100000E+02    4.200000E+02    -0.             -0.             -0.
    3  4.500000E+01    4.000000E+02    0.              -0.             -0.             -0.
```

Table A-4. OUT1 Subroutine Output—Problem of Figure 12.

```
PROBLEM DUCT  123   NCFL=  09/17/73
CYCLE   TIME(SEC)     NEXT TIMESTEP   IPT    JPT
  500   4.92974E-03   4.92e79E-0A       2     19


      PS              QS            TEMPS           ZS            GAMMAS          HTS           DS            ES

 5.21912?0E+07  1.1535955E+0A  3.19310?6E+03  1.0131148E+00  1.2984638E+00  6.0924471E+1?  5.62e5473E-03  3.1114059E+1?


 I   J  X(I,J+1)    U(I,J+1)   X CENTER  DENSITY    ENERGY     PQ(I,J)    Q(I,J)  PRESSURE   ZONE MASS   TEMP      DT/J      GAM      Z
          CM         CM/SEC       CM      GM/CC     ERG/GM   DYNE/SQCM DYNE/SQCM   PSIA       GRAMS     KELVIN      SEC
 0   0 2.55256E+01 1.211E-05-0.          -0.        4.269E+1?1.479E+07-0.          2.144E+02
 1   1 2.31731E+01 1.?68E+05 3.935E+01 1.368E-03 4.213E+1? 1.497E+07 8.14E+04 2.170E+02 1.069E+02 3.688E+03 1.?0E-04 1.26 1.042E+00
 1   2 2.07629E+01 1.144E+05 6.672E+01 1.395E-03 4.184E+1? 1.540E+07 8.08E+05 2.218E+02 1.069E+02 3.669E+03 1.07E-04 1.26 1.041E+00
 1   3 1.86009E+02 1.139E+05 9.314E+01 1.458E-03 4.177E+1? 1.624E+07 2.94E+05 2.319E+02 1.061E+02 3.670E+03 8.75E-05 1.26 1.041E+00
 1   4 1.29900E+02 1.086E+05 1.180E+02 1.545E-03 4.187E+1? 1.735E+07 3.51E+05 2.445E+02 1.044E+02 3.681E+03 7.65E-05 1.26 1.041E+00
 1   5 1.52672E+02 1.036E+05 1.412E+02 1.644E-03 4.204E+1? 1.851E+07 3.62E+05 2.635E+02 1.040E+02 3.696E+03 7.37E-05 1.26 1.042E+00
 1   6 1.73960E+02 1.000E+05 1.632E+02 1.739E-03 4.216E+1? 1.951E+07 2.26E+05 2.707E+02 1.057E+02 3.708E+03 7.73E-05 1.26 1.042E+00
 1   7 1.95143E+02 9.842E+04 1.846E+02 1.811E-03 4.212E+1? 2.019E+07 8.54E+04 2.819E+02 1.085E+02 3.714E+03 8.45E-05 1.26 1.042E+00
 1   8 2.15?22E+02 9.861E+04 2.051E+02 1.852E-03 4.196E+1? 2.048E+07 0.          2.978E+02 1.041E+02 3.699E+03 9.45E-05 1.26 1.041E+00
 1   9 2.34050E+02 1.002E+05 2.255E+02 1.863E-03 4.146E+1? 2.044E+07 0.          2.978E+02 1.103E+02 3.688E+03 8.77E-05 1.27 1.040E+00
 1  10 2.54089E+02 1.016E+05 2.465E+02 1.864E-03 4.098E+1? 2.032E+07 0.          2.948E+02 1.109E+02 3.655E+03 9.07E-05 1.27 1.039E+00
 1  11 2.74257E+02 1.022E+05 2.674E+02 1.877E-03 4.059E+1? 2.035E+07 0.          2.951E+02 1.129E+02 3.636E+03 9.78E-05 1.27 1.039E+00
 1  12 2.97683E+02 1.032E+05 2.880E+02 1.892E-03 4.019E+1? 2.038E+07 0.          2.954E+02 1.139E+02 3.614E+03 8.68E-05 1.27 1.038E+00
 1  13 3.17442E+02 1.042E+05 3.076E+02 1.899E-03 3.983E+1? 2.034E+07 0.          2.950E+02 1.061E+02 3.598E+03 8.82E-05 1.27 1.037E+00
 1  14 3.37533E+02 1.049E+05 3.275E+02 1.914E-03 3.949E+1? 2.033E+07 0.          2.949E+02 1.085E+02 3.581E+03 9.24E-05 1.27 1.036E+00
 1  15 3.57929E+02 1.055E+05 3.477E+02 1.925E-03 3.916E+1? 2.038E+07 0.          2.956E+02 1.110E+02 3.564E+03 9.55E-05 1.27 1.035E+00
 1  16 3.78493E+02 1.046E+05 3.683E+02 1.947E-03 3.888E+1? 2.058E+07 4.20E+04 2.978E+02 1.139E+02 3.551E+03 9.43E-05 1.27 1.035E+00
 1  17 3.97842E+02 1.012E+05 3.878E+02 2.006E-03 3.878E+1? 2.138E+07 2.43E+05 3.084E+02 1.184E+02 3.549E+03 8.82E-05 1.27 1.034E+00
 1  18 4.15458E+02 9.821E+04 4.063E+02 2.107E-03 3.886E+1? 2.270E+07 4.38E+05 3.230E+02 1.204E+02 3.559E+03 8.09E-05 1.27 1.035C+00
 1  19 4.31490E+02 9.644E+04 4.237E+02 2.222E-03 3.902E+1? 2.378E+07 1.48E+05 3.429E+02 1.041E+02 3.571E+03 8.71E-05 1.27 1.035F+00
 1  20 4.5?000E+02 9.782E+04 4.410E+02 2.229E-03 3.848E+1? 2.363E+07 0.          3.398E+02 1.139E+02 3.542E+03 8.49E-05 1.27 1.034E+00
```

continued

Table A-4. Continued

DUCT NZONES
1 20

MAXIMUM Q OF AREA 1 IS IN ZONE 18 AT R= 6.0639E+02
MAXIMUM PSI OF AREA 1 IS IN ZONE 19 AT R= 6.2372E+02

I	J	R[I,J+1] CM	U[I,J+1] CM/SEC	R CENTER CM	DENSITY GM/CC	ENERGY ERG/GM	PQ[I,J] DYNE/SQCM	Q[I,J] DYNE/SQCM	PRESSURE PSIA	ZONE MASS GRAMS	TEMP KELVIN	DTJ SEC	GAM	Z
1	0	0.	1.0000E+05	0.	0.	3.0000E+10	1.0000E+07	0.	2.0000E+02					
2	1	1.0000E+01	1.0000E+05	5.0000E+00	1.0000E-03	3.0000E+10	1.0000E+07	0.	2.0000E+02	5.0000E+00	3.0000E+01	1.0000E-05	1.67	1.0000E+00
2	2	2.0000E+01	1.0000E+05	1.5000E+01	1.0000E-03	3.0000E+10	1.0000E+07	0.	2.0000E+02	1.5000E+01	3.0000E+01	1.0000E-05	1.67	1.0000E+00
2	3	3.0000E+01	1.0000E+05	2.5000E+01	1.0000E-03	3.0000E+10	1.0000E+07	0.	2.0000E+02	2.5000E+01	3.0000E+01	1.0000E-05	1.67	1.0000E+00
2	4	4.0000E+01	1.0000E+05	3.5000E+01	1.0000E-03	3.0000E+10	1.0000E+07	0.	2.0000E+02	3.5000E+01	3.0000E+01	1.0000E-05	1.67	1.0000E+00
2	5	5.0000E+01	1.0000E+05	4.5000E+01	1.0000E-03	3.0000E+10	1.0000E+07	0.	2.0000E+02	4.5000E+01	3.0000E+01	1.0000E-05	1.67	1.0000E+00
2	6	6.0000E+01	1.0000E+05	5.5000E+01	1.0000E-03	3.0000E+10	1.0000E+07	0.	2.0000E+02	5.5000E+01	3.0000E+01	1.0000E-05	1.67	1.0000E+00
2	7	7.0000E+01	1.0000E+05	6.5000E+01	1.0000E-03	3.0000E+10	1.0000E+07	0.	2.0000E+02	6.5000E+01	3.0000E+01	1.0000E-05	1.67	1.0000E+00
2	8	8.0000E+01	1.0000E+05	7.5000E+01	1.0000E-03	3.0000E+10	1.0000E+07	0.	2.0000E+02	7.5000E+01	3.0000E+01	1.0000E-05	1.67	1.0000E+00
2	9	9.0000E+01	1.0000E+05	8.5000E+01	1.0000E-03	3.0000E+10	1.0000E+07	0.	2.0000E+02	8.5000E+01	3.0000E+01	1.0000E-05	1.67	1.0000E+00
2	10	1.0000E+02	1.0000E+05	9.5000E+01	1.0000E-03	3.0000E+10	1.0000E+07	0.	2.0000E+02	9.5000E+01	3.0000E+01	1.0000E-05	1.67	1.0000E+00
2	11	1.1000E+02	1.0000E+05	1.0500E+02	1.0000E-03	3.0000E+10	1.0000E+07	0.	2.0000E+02	1.0500E+02	3.0000E+01	1.0000E-05	1.67	1.0000E+00
2	12	1.2000E+02	1.0000E+05	1.1500E+02	1.0000E-03	3.0000E+10	1.0000E+07	0.	2.0000E+02	1.1500E+02	3.0000E+01	1.0000E-05	1.67	1.0000E+00
2	13	1.3000E+02	1.0000E+05	1.2500E+02	1.0000E-03	3.0000E+10	1.0000E+07	0.	2.0000E+02	1.2500E+02	3.0000E+01	1.0000E-05	1.67	1.0000E+00
2	14	1.4000E+02	1.0000E+05	1.3500E+02	1.0000E-03	3.0000E+10	1.0000E+07	0.	2.0000E+02	1.3500E+02	3.0000E+01	1.0000E-05	1.67	1.0000E+00
2	15	1.5000E+02	1.0000E+05	1.4500E+02	1.0000E-03	3.0000E+10	1.0000E+07	0.	2.0000E+02	1.4500E+02	3.0000E+01	1.0000E-05	1.67	1.0000E+00
2	16	1.6000E+02	1.0000E+05	1.5500E+02	1.0000E-03	3.0000E+10	1.0000E+07	0.	2.0000E+02	1.5500E+02	3.0000E+01	1.0000E-05	1.67	1.0000E+00
2	17	1.7000E+02	1.0000E+05	1.6500E+02	1.0000E-03	3.0000E+10	1.0000E+07	0.	2.0000E+02	1.6500E+02	3.0000E+01	1.0000E-05	1.67	1.0000E+00
2	18	1.8000E+02	1.0000E+05	1.7500E+02	1.0000E-03	3.0000E+10	1.0000E+07	0.	2.0000E+02	1.7500E+02	3.0000E+01	1.0000E-05	1.67	1.0000E+00
2	19	1.8500E+02	1.0000E+05	1.8250E+02	1.0000E-03	3.0000E+10	1.0000E+07	0.	2.0000E+02	9.1250E+01	3.0000E+01	1.0000E-05	1.67	1.0000E+00
2	20	1.9000E+02	1.0000E+05	1.8750E+02	1.0000E-03	3.0000E+10	1.0000E+07	0.	2.0000E+02	9.3750E+01	3.0000E+01	1.0000E-05	1.67	1.0000E+00
2	21	1.9250E+02	1.0000E+05	1.9125E+02	1.0000E-03	3.0000E+10	1.0000E+07	0.	2.0000E+02	4.7812E+01	3.0000E+01	1.0000E-05	1.67	1.0000E+00
2	22	1.9500E+02	1.0000E+05	1.9375E+02	1.0000E-03	3.0000E+10	1.0000E+07	0.	2.0000E+02	4.8438E+01	3.0000E+01	1.0000E-05	1.67	1.0000E+00
2	23	1.9750E+02	1.0000E+05	1.9625E+02	1.0000E-03	3.0000E+10	1.0000E+07	0.	2.0000E+02	4.9062E+01	3.0000E+01	1.0000E-05	1.67	1.0000E+00
2	24	1.9944E+02	1.0000E+05	1.9847E+02	1.0000E-03	3.0000E+10	1.0000E+07	0.	2.0000E+02	4.9559E+01	3.0000E+01	1.0000E-05	1.67	1.0000E+00
2	25	2.0000E+02	1.0000E+05	1.9972E+02	1.0000E-03	3.0000E+10	1.0000E+07	0.	2.0000E+02	4.9874E+01	3.0000E+01	1.0000E-05	1.67	1.0000E+00
2	26	2.0056E+02	1.0000E+05	2.0028E+02	1.0000E-03	3.0000E+10	1.0000E+07	0.	2.0000E+02	5.0031E+01	3.0000E+01	1.0000E-05	1.67	1.0000E+00
2	27	2.0167E+02	1.0000E+05	2.0111E+02	1.0000E-03	3.0000E+10	1.0000E+07	0.	2.0000E+02	5.0278E+01	3.0000E+01	1.0000E-05	1.67	1.0000E+00
2	28	2.0278E+02	1.0000E+05	2.0222E+02	1.0000E-03	3.0000E+10	1.0000E+07	0.	2.0000E+02	5.0556E+01	3.0000E+01	1.0000E-05	1.67	1.0000E+00
2	29	2.0389E+02	1.0000E+05	2.0333E+02	1.0000E-03	3.0000E+10	1.0000E+07	0.	2.0000E+02	5.0833E+01	3.0000E+01	1.0000E-05	1.67	1.0000E+00
2	30	2.0500E+02	1.0000E+05	2.0444E+02	1.0000E-03	3.0000E+10	1.0000E+07	0.	2.0000E+02	5.1111E+01	3.0000E+01	1.0000E-05	1.67	1.0000E+00
2	31	2.0611E+02	1.0000E+05	2.0556E+02	1.0000E-03	3.0000E+10	1.0000E+07	0.	2.0000E+02	5.1389E+01	3.0000E+01	1.0000E-05	1.67	1.0000E+00
2	32	2.0722E+02	1.0000E+05	2.0667E+02	1.0000E-03	3.0000E+10	1.0000E+07	0.	2.0000E+02	5.1667E+01	3.0000E+01	1.0000E-05	1.67	1.0000E+00
2	33	2.0833E+02	1.0000E+05	2.0778E+02	1.0000E-03	3.0000E+10	1.0000E+07	0.	2.0000E+02	5.1944E+01	3.0000E+01	1.0000E-05	1.67	1.0000E+00
2	34	2.0944E+02	1.0000E+05	2.0889E+02	1.0000E-03	3.0000E+10	1.0000E+07	0.	2.0000E+02	5.2222E+01	3.0000E+01	1.0000E-05	1.67	1.0000E+00
2	35	2.1056E+02	1.0000E+05	2.1000E+02	1.0000E-03	3.0000E+10	1.0000E+07	0.	2.0000E+02	5.2500E+01	3.0000E+01	1.0000E-05	1.67	1.0000E+00
2	36	2.1167E+02	1.0000E+05	2.1111E+02	1.0000E-03	3.0000E+10	1.0000E+07	0.	2.0000E+02	5.2778E+01	3.0000E+01	1.0000E-05	1.67	1.0000E+00
2	37	2.1278E+02	1.0000E+05	2.1222E+02	1.0000E-03	3.0000E+10	1.0000E+07	0.	2.0000E+02	5.3056E+01	3.0000E+01	1.0000E-05	1.67	1.0000E+00
2	38	2.1389E+02	1.0000E+05	2.1333E+02	1.0000E-03	3.0000E+10	1.0000E+07	0.	2.0000E+02	5.3333E+01	3.0000E+01	1.0000E-05	1.67	1.0000E+00
2	39	2.1500E+02	1.0000E+05	2.1444E+02	1.0000E-03	3.0000E+10	1.0000E+07	0.	2.0000E+02	5.3611E+01	3.0000E+01	1.0000E-05	1.67	1.0000E+00
2	40	2.1611E+02	1.0000E+05	2.1556E+02	1.0000E-03	3.0000E+10	1.0000E+07	0.	2.0000E+02	5.3889E+01	3.0000E+01	1.0000E-05	1.67	1.0000E+00
2	41	2.1722E+02	1.0000E+05	2.1667E+02	1.0000E-03	3.0000E+10	1.0000E+07	0.	2.0000E+02	5.4167E+01	3.0000E+01	1.0000E-05	1.67	1.0000E+00
2	42	2.1833E+02	1.0000E+05	2.1778E+02	1.0000E-03	3.0000E+10	1.0000E+07	0.	2.0000E+02	5.4444E+01	3.0000E+01	1.0000E-05	1.67	1.0000E+00
2	43	2.1944E+02	1.0000E+05	2.1889E+02	1.0000E-03	3.0000E+10	1.0000E+07	0.	2.0000E+02	5.4722E+01	3.0000E+01	1.0000E-05	1.67	1.0000E+00

continued

Table A-4. Continued

DUCT NZONES
2 51

MAXIMUM Q OF AREA 2 IS IN ZONE 36 AT R= 1.944BE+02
MAXIMUM PSI OF AREA 2 IS IN ZONE 1 AT R= 8.1A08E+00

I	J	R(I,J,1) CM	U(I,J,1) CM/SEC	R CENTER CM	DENSITY GM/CC	ENERGY ERG/GM	PHI(I,J) DYNE/SQCM	QT(I,J) DYNE/SQCM	PRESSURE PSIA	ZONE MASS GRAMS	TEMP KELVIN	DTJJ SEC	GAM	Z
2	0	0.	2.944E+04	0.	-0.	6.A51E+19	6.923E+0A	-0.	1.004E+02					
3	1	7.38[illegible]7E+01	5.1A5E+04	3.A91E+01	8.173E+00	2.173E+19	6.6A3E+0A	0.	8.124E+01	1.704E+02	2.389E+03	1.26E-04	1.37	1.000E+00
3	2	9.82A31E+01	4.157E+04	8.A01E+01	1.50AE+01	1.203E+19	6.A47E+06	0.	9.059E+01	1.A4AE+02	1.586E+03	7.A2E-05	1.35	1.000E+00
3	3	1.139[illegible]6E+02	4.49AE+04	1.A01E+02	2.93AE+01	9.372E+0A	6.A58E+0A	0.	1.168E+02	1.A39E+02	1.20AE+03	8.A8E-05	1.37	1.000E+00
3	4	1.224A0E+02	4.410E+04	1.182E+02	4.31AE+01	8.A20E+09	8.236E+06	4.79E+0A	1.198E+02	1.039E+02	6.A14E+02	7.99E-05	1.39	1.000E+00
3	5	1.317A1E+02	5.7A2E+04	1.271E+02	3.43AE+01	6.562E+09	7.A26E+0A	8.12E+05	1.A17E+02	1.039E+02	6.205E+02	6.A8E-05	1.39	1.000E+00
3	6	1.44A71E+02	6.544E+04	1.376E+02	2.99AE+01	5.A12E+09	6.A78E+0A	2.07E+06	4.69AE+01	1.039E+02	5.378E+02	3.76E-05	1.39	1.000E+00
3	7	1.611A1E+02	2.95AE+04	1.A20E+02	2.15AE+01	3.12AE+09	6.A45E+0A	2.28E+06	3.095E+01	1.039E+02	4.345E+02	4.37E-05	1.40	1.000E+00
3	8	1.A7A12E+02	1.43AE+04	1.72AE+02	1.A3AE+01	2.5A5E+09	3.225E+0A	1.A9E+06	2.377E+01	1.039E+02	3.A91E+02	6.A8E-05	1.40	1.000E+00
3	9	2.1[illegible]A1E+02	3.A02E+03	1.971E+02	1.341E+01	2.184E+09	1.A3AE+06	6.A9E+05	1.724E+01	1.039E+02	3.043E+02	1.A0E-04	1.40	1.000E+00
3	10	2.A[illegible]4E+02	3.5A6E+02	2.25AE+02	1.24AE+01	2.A85E+09	1.13AE+06	8.A2E+04	1.511E+01	1.039E+02	2.905E+02	2.25E-04	1.40	1.000E+00
3	11	2.7A0E1E+02	1.33AE+01	2.550E+02	1.227E+01	2.A49E+09	1.01AE+06	3.32E+03	1.472E+01	1.039E+02	2.A83E+02	4.52E-04	1.40	1.000E+00
3	12	3.[illegible]A0E+02	2.7A5E+01	2.A50E+02	1.225E+01	2.A48E+09	1.013E+06	1.07E+02	1.470E+01	1.039E+02	2.A82E+02	5.A2E-04	1.40	1.000E+00
3	13	3.3A0A0E+02	0.	3.15[illegible]E+02	1.225E+01	2.A48E+09	1.013E+06	2.23E+A0	1.470E+01	1.039E+02	2.A82E+02	5.A4E-04	1.40	1.000E+00
3	14	3.6A0A0E+02	0.	3.65AE+02	1.225E+01	2.A48E+09	1.013E+06	0.	1.470E+01	1.039E+02	2.A82E+02	5.A4E-04	1.40	1.000E+00
3	15	3.9A0A0E+02	0.	3.75AE+02	1.225E+01	2.A48E+09	1.013E+06	0.	1.470E+01	1.039E+02	2.A82E+02	5.A4E-04	1.40	1.000E+00
3	16	4.2A0A0E+02	0.	4.05AE+02	1.225E+01	2.A48E+09	1.013E+06	0.	1.470E+01	1.039E+02	2.A82E+02	5.A4E-04	1.40	1.000E+00

DUCT NZONES
3 52

MAXIMUM Q OF AREA 3 IS IN ZONE 7 AT R= 1.A6A9E+02
MAXIMUM PSI OF AREA 3 IS IN ZONE 6 AT R= 1.1B19E+02

Table A-5. OUT1 Subroutine Printout Variables

Printout Variable	Description
IDT	Duct with smallest time step
JDT	Zone with smallest time step
PS	Surface pressure
QS	Surface dynamic pressure
TEMPS	Surface temperature
ZS	Surface compressibility factor
GAMMAS	Surface value of gamma
HTS	Surface value of total enthralpy
DS	Surface density
ES	Surface internal energy
I	Number of duct
J	Number of interface
X(I, J)	Distance to interface
U(I, J)	Velocity of interface
XAV(I, J)	Distance to zone center
D(I, J)	Density
E(I, J)	Internal energy
PQ(I, J)	P + Q
Q(I, J)	Pseudo-viscosity
P(I, J)	Pressure
GRAMS(I, J)	Zone mass
TEMP(I, J)	Temperature
DIA(I, J)	Duct diameter
DTZJ(I, J)	Time step in duct I at zone J
GAMMA(I, J)	Adiabatic exponent gamma
ZJ(I, J)	Compressibility factor

Table A-6. OUT3 Subroutine Printout Variables

Printout Variables	Description
I	Duct number
S(I, J)	Positions P-T data collected
NCYCLE	Number of computation cycles
T	Real problem time
PSI(I, J)	Pressure, psia
OVPSI(I, J)	Overpressure, psi
PDYN(I, J)	Dynamic pressure, psi
D(I, J)	Density
U(I, J)	Velocity of interface
TEMP(I, J)	Temperature

Appendix B

EULERIAN COMPUTER CODE INPUT AND OUTPUT PARAMETERS

The input and output parameters are presented for the Eulerian computer code. A tape of the code for listing and card punching is available upon request from the Computer Center, Code 1.06, CEL.

COMPUTER CODE INPUT PARAMETERS

The input parameters are listed in Table B-1.

Table B-1. Eulerian Code Input Parameters

Symbol	Definition
PO	Ambient pressure, $lb/in.^2$
TO	Ambient temperature, ^{O}R
RO	Ambient specific gas constant, $ft/^{O}F$
GO	Ambient specific heat ratio
R2	High temperature specific gas constant, $ft/^{O}F$
G2	High temperature specific heat ratio
A1(i), A2(i), A3(i), A4(i); i = 1, 4	Constants in equation for duct radius in duct section i, $r(i) = A1(i) + A2(i)\,x + A3(i)\,x^2 + A4(i)\,x^3$; all zero except A1(1) for listing given in Appendix B.
XB(1), XB(2), XB(3)	Maximum x values in the 1st, 2nd, and 3rd sections of the duct; all greater than XFIN for listing given in Appendix B.
B1, B2, B3, B4	Constants in the equation for overpressure transmitted into the duct; $p(0,0) = p_a + B1(p_s - p_a)^{B2}$; (B3 and B4 are not currently used)
XIN	X value at duct entrance; use XIN = 0
XFIN	X value at end of duct, ft
DELX	Δx, finite-difference mesh size, ft
A	Mach number of nuclear blast wave as it passes over duct entrance
ALPHA	t_i, time constant; $p(0,t) = p_a + [p(0,0) - p_a]e^{-t/t_i}$
BETA	Not used
S1, S2	Constants used in computing friction factor, f; $f = S1(R_e)^{S2}$

continued

Table B-2. Continued

Symbol	Definition
XXIY	F, constant used in computing time increment; $\Delta t = \Delta x/F(U + C)$
K1, K2, K3	Constants used in the computation of the pseudo-viscosity factors, usually 2.0
ID	= 1, if duct is rectangle of unit width
	= 2, if duct is circular
IY	Not used
NEND	Initializing parameter, set NEND = 1
NTIME	Maximum value of n, i.e., number of time steps to be computed
IWRTTP	Output is printed every IWRTTPth time step
IWRTXP	Output is printed every IWPTXPth space step for every IWRTTPth time step
NF	= 0, if friction factor, f, is zero
	= 1, if friction factor, f, is computed from $f = S1(R_e)^{S2}$
ITL	Number of time steps that must be computed before the pseudo-viscosity factors take on their full value; for $n < ITL$, the pseudo-viscosity factors are proportional to n/ITL
NWRT	The maximum value of pressure at a given value of axial distance; printed out every NWRTth space step
IWP	Properties behind the nuclear blast wave; printed out every IWPth time step

COMPUTER CODE OUTPUT PARAMETERS

The output parameters are listed in Table B-2.

Table B-2. Eulerian Code Output Parameters

Symbol	Definition
TIME	Elapsed time from appearance of shock wave at duct entrance, sec
X	Axial distance, ft

continued

Table B-2. Continued

Symbol	Definition
X/L	Nondimensional axial distance, normalized with respect to duct length
RHO	Density, lbm/ft^3
Y	Duct radius of half-height, ft
Y/Y1	Nondimensional duct radius or half-height, normalized with respect to initial value
U	Velocity, ft/sec
AREA	Duct area, ft^2
AREA/AREA1	Nondimensional duct area, normalized with respect to initial value
MACH NO	Mach number
P	Pressure, lb/in.^{2}
P/PO	Nondimensional pressure, normalized with respect to ambient value
RHO/RHO	Nondimensional density, normalized with respect to ambient value
T	Temperature, ^{O}F
T/TO	Nondimensional temperature, normalized with respect to ambient value
I	Number of space increment
X(I)	Value of X at the Ith space increment, ft
X/D	Nondimensional axial distance, normalized with respect to initial duct diameter or height
P/PO	Maximum value of nondimensional pressure at X(I), normalized with respect to ambient value
P	Maximum value of pressure at X(I), lb/in.^{2}

BASIC NOMENCLATURE

A	Duct cross-sectional area
A_1–A_5	Constants, Lagrange Code
a	Acceleration
a_1, a_2	Pseudo-viscosity constants, Lagrange Code
b_1–b_5	Constants, Lagrange Code
c	Acoustic velocity
D	Duct diameter
D_p^+	Duration of positive pressure phase, nuclear wave
D_u^+	Duration of positive velocity phase, nuclear wave
e	Specific internal energy
E	Variable defined as $\rho(e + 1/2u^2)$
F	Stability constant, Eulerian Code
$F(U)$	Function of vector U
f	Friction factor
g_0^+	Pseudo-viscosity factor, Eulerian Code
g_1^+	Pseudo-viscosity factor, Eulerian Code
g_2^+	Pseudo viscosity factor, Eulerian Code
g_0^-	Pseudo-viscosity factor, Eulerian Code
g_1^-	Pseudo-viscosity factor, Eulerian Code
g_2^-	Pseudo-viscosity factor, Eulerian Code
$G(U)$	Function of vector U
h	Specific enthalpy

h_t	Total enthalpy per unit mass
H	Duct hydraulic radius
K_1, K_2, K_3	Pseudo-viscosity constant, Eulerian Code
L	Duct length
m	Lagrange variable, mass per zone
Δm	Mass change per zone, Lagrange Code
M_s	Shock wave Mach number
M	Variable defined as ρ u A, Eulerian Code
N	Variable defined as ρ A, Eulerian Code
p	Pressure
p(x,t)	Pressure at position x at time t
P	Variable defined as p + q, Lagrange Code
q	Pseudo-viscosity, Lagrange Code
Q	Dynamic pressure
R	Particular gas constant
R_e	Reynolds number
S_1, S_2	Friction factor constants, Eulerian Code
S	Specific entropy
t	Time
t_s	Shock arrival time
t_i	Initial slope time intercept
Δt	Time increment
u	Particle velocity
u_s	Shock wave velocity
U	Variable vector, Eulerian Code

V	Volume per unit mass
x	Distance along duct, Eulerian variable
Δx	Distance increment
Z	Compressibility factor for real gas
$\alpha_1, \alpha_2, \alpha_3$	Pseudo-viscosity parameter, Eulerian Code
γ	Adiabatic exponent
ζ	Small quantity
μ^2	Defined as $(\gamma - 1)/(\gamma + 1)$
ρ	Density
$\rho(x,t)$	Density at position x at time t
τ	Defined as $(t - t_s)/D_p^*$
τ_w	Shear stress at wall of duct
ω	Defined as $(t - t_s)/D_u^*$

Subscripts

1	Downstream of shock
2	Upstream of shock
a	Ambient condition value
e	Duct inlet value
j	Net point location
o	Initial value
s	Surface value

Superscripts

n	Number of time increments